THE OPTIMUM USE OF CONIFEROUS TREES IN REDUCING HOME ENERGY CONSUMPTION

by

C. E. Buckley
D. T. Harrje
M. P. Knowlton

Princeton University

and

G. M. Heisler

Northeast Forest Experiment Station

the center for environmental studies

princeton university
princeton, new jersey

THE OPTIMUM USE OF CONIFEROUS TREES IN REDUCING HOME ENERGY CONSUMPTION

by

C. E. Buckley
D. T. Harrje
M. P. Knowlton

Princeton University

and

G. M. Heisler

Northeast Forest Experiment Station

Report PU/CES 71

May 1978

Research Sponsored by the
Pinchot Consortium for Environmental Forestry Studies
Grant No. 23-758

Center for Environmental Studies
The Engineering Quadrangle
Princeton University
Princeton, N. J. · 08540

ACKNOWLEDGEMENT

The authors wish to gratefully acknowledge the assistance to the project rendered by the staff of the Princeton University Subsonics Laboratory, where the testing was conducted. This aid was often above and beyond the call of duty, especially that rendered by Mr. William James and Mr. Robert Kneeshaw.

Many thanks go to the staff of the Northeastern Forest Experiment Station, who provided much of the background material for the work.

The testing was conducted with the assistance of Mr. Glenn Bryce and Mr. Roland Neaves. Thanks go to Ms. Gail Hadden for her demonstration of the digitizing system.

This research was supported in part by funds provided by the Northeastern Forest Experiment Station through the Pinchot Institute of Environmental Forestry Research, Consortium for Environmental Forestry Studies.

ABSTRACT

Work carried out by Mattingly, Peters, Harrje and Heisler at Princeton University's Center for Environmental Studies in early 1975 indicated that there exists significant possibility for reduction of winter home heating energy consumption through reduction of air infiltration into the home by using sheltering devices such as fences, neighboring buildings, and trees.

In this study, a wind tunnel air infiltration model developed by Mattingly and Peters is used to explore more extensively the effects of trees in a windbreak on a model home. It was desired to determine the optimum planting arrangement for windbreak coniferous trees to yield the maximum reduction of wind-induced air infiltration in the home.

Results of tests determining the effect on wind-induced air infiltration of the variation of various windbreak layout parameters are presented. The concept of turbulence generation as the mechanism of tree wind sheltering is introduced.

It is concluded that windbreaks are an economically viable method of reducing home energy consumption. A method for predicting monetary savings due to the planting of a windbreak is outlined, and an example of its use is given.

TABLE OF CONTENTS

1. INTRODUCTION

Studies of winter home heating energy consumption at the Twin Rivers Planned Unit Development located in West Windsor, N. J. have indicated that there are three ways in which heating energy is dissipated into the outside environment. The three categories and the percentage of total heat loss attributable to each are shown in Figure 1(1), where the categories form proportionate slices in the heat loss pie. In the "Windows" and the "Conduction - Walls and Ceiling" categories, the heat loss rates are controlled mainly by the thermal conductivity of the materials which form the shell of the house, and there is only a small dependence on pressure and/or velocity conditions of the air next to the shell surfaces.

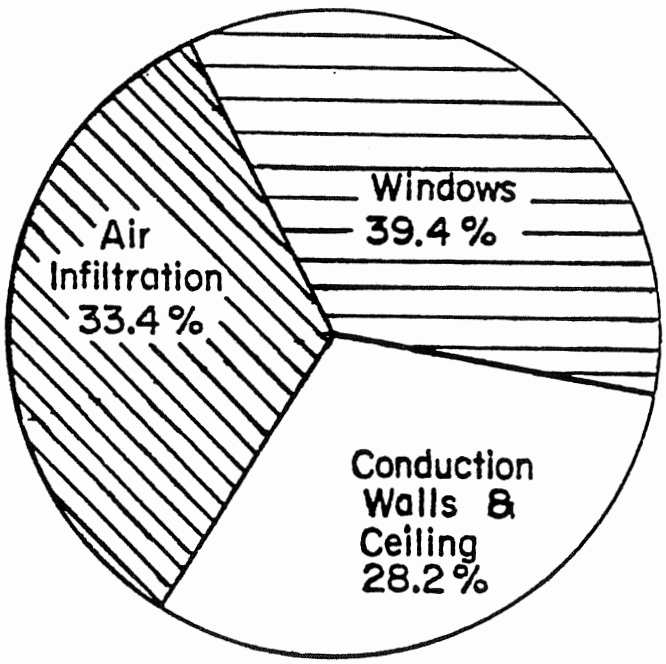

Figure 1: Winter Home Heat Loss Categories for an Average Twin Rivers Townhouse

---

1. Harrje, D. T. "Retrofitting: Plan, Action, and Early Results at Twin Rivers", C. E. S. Report No. 29, June 1976, Fig. 4

The "Air Infiltration" category represents in magnitude an average of infiltration rates observed at Twin Rivers. At ambient windspeeds of over 20 mph, the percentage of air infiltration contribution to total heat loss has risen as high as 60%(2). The rate of heat loss due to air infiltration is controlled by the porosity of the house shell. This porosity is due to flow through cracks in walls where material is loosely joined, through intended openings in the house shell, and directly through porous building material.

It is undesirable to eliminate air infiltration entirely in a house, as this would cut off the supplying of fresh air to its occupants. Reduction of air infiltration is, however, a worthwhile goal. As compared to the air infiltration rate represented by the 33.4% heat loss contribution figure given above, air infiltration rates 6 times as high have been observed in high winds, and rates 1/3 as high have been seen with no adverse effects on the occupants(3). Thus, there is room for substantial reduction and heat savings. Reduction of air infiltration certainly does not preclude its voluntary increase by the occupants of the house, by opening a window, for example.

Air infiltration is driven by a pressure drop across the surface of a house. Such a pressure drop is induced in two ways. One is due to the buoyant effects of the house interior air. The interior air volume of a house is divided into subvolumes by rooms. Although ideal living space conditions are nearly always thought of as a uniform 68 degrees Fahrenheit, there are a number of small air pockets at various points about any room whose temperatures vary over a range about the ideal one. In time, the warmer air pockets will float up towards the ceiling of the room, being pushed upward by the buoyant forces of the relatively heavier colder pockets. Thus, a pressure gradient is set up within the room, with higher pressure at the ceiling than at the floor. If one of the room walls is an exterior wall, even if there is no wind outside the house, the pressure gradient will draw outside air in through the wall pores near the floor and push air out through the wall pores near the ceiling. This lowers the net temperature in the house, the thermostat on the heater responds, and the air is warmed back up. The process repeats perpetually. This air infiltration due to the thermal pressure gradient has been traditionally called "the stack effect". The stack effect has been observed to account for about 25% of home air infiltration in a wind-exposed situation.

---

2. Harrje, p. 8

3. Mattingly, G. E., and Peters, E. F., "Wind and Trees - Air Infiltration Effects on Energy in Housing", Center for Environmental Studies Report No. 20, May 1975, p. 9

Ambient wind conditions about a house also induce pressure differences across its exterior surfaces. Wind accounts for the other 75% of home air infiltration. This study is concerned with the reduction of wind-induced air infiltration.

Trees have traditionally been used to shelter buildings, roads, and fields. This is especially true of the midwestern United States, where the windbreak plays a key role in agriculture. Mattingly, Harrje, and Heisler have shown by placing actual full-size trees in front of a Twin Rivers townhouse, and comparing measured air infiltration rates for the sheltered and unsheltered cases that an air infiltration reduction of up to 60% may be achieved(4). Mattingly and Peters predicted a wind-induced air infiltration reduction into their 1/48th scale model Twin Rivers townhouse subjected to wind conditions in a wind tunnel by placement of an upstream row of 2-dimensional model trees. The usefulness of trees for climatic protection of homes is an established fact.

The purpose of this study is to determine how to plant trees to afford optimum wind protection, i. e. the maximum wind protection of a home for the number of tree dollars spent. This is accomplished through simulation of various trees/house configurations in a wind tunnel, since an analytic study would require a solution of the full turbulent Navier-Stokes equation, an undertaking of enormous complexity(5). This study deals with such factors as size and thickness of trees, tree windbreak shape, distance from windbreak to sheltered building, angle of approach of wind, the sheltering value of leeward and neighboring trees, and the effect of natural pruning. A technique for applying the experimental results to windbreak planning is given.

---

4. Mattingly, G. E., Harrje, D. T., and Heisler, G. M., "On the Effectiveness of Evergreen Windbreaks for Reducing Residential Energy Consumption", CES Draft Report, August 1977

5. Plate, E. J., Aerodynamic Characteristics of Atmospheric Boundary Layers, AEC Critical Review Series, Oak Ridge, 1972, p. 161

2. EXPERIMENTAL PROCEDURE

Two types of tests were conducted in this study. The main thrust of the experimental findings are based upon tests involving a model house outfitted to measure local pressure at various points on its exterior, and scale model trees configured in various ways in simulated planetary surface windflow. These tests used a variation of the Mattingly/Peters wind-induced air infiltration quantification technique to calculate an index of wind-induced air infiltration called the AI parameter. The variations of this parameter were observed over a range of tests so designed as to indicate the effect on wind-induced air infiltration of the variation of a single windbreak arrangement parameter, such as tree height, house-to-windbreak distance, etc. When these tests, called the force tunnel tests after the wind tunnel in which they were performed, indicated that there might be a particularly interesting phenomenon behind a particuler AI result, a smoke tunnel test was conducted on a similar house and tree configuration to visually identify the phenomenon.

2.1 SMOKE TUNNEL TESTS

The smoke tunnel tests were conducted in a three-dimensional smoke study wind tunnel, designed to provide smoothly flowing air. In these tests, a house and tree configuration was placed in the smoke tunnel, and the wind was turned on. Then, by means of a non-obstructive pipe with three small nozzles, a flow of vaporized kerosene smoke was introduced into the airstream at some point of interest. By observing the shape of the smoke stream formed, it was possible to determine the path of the streamlines which passed through the point of smoke introduction. The best medium for the presentation of the qualitative information obtained from these tests is photography, so the smoke tunnel experimental installation included a Polaroid camera to photograph the tests. Photographs of key effects are exhibited in the text as appropriate. A sample test photograph is shown in Figure 2.

In this report, a photograph of dark colored houses and trees depicts a smoke tunnel test, while a photograph of light colored houses and trees depicts a force tunnel test configuration.

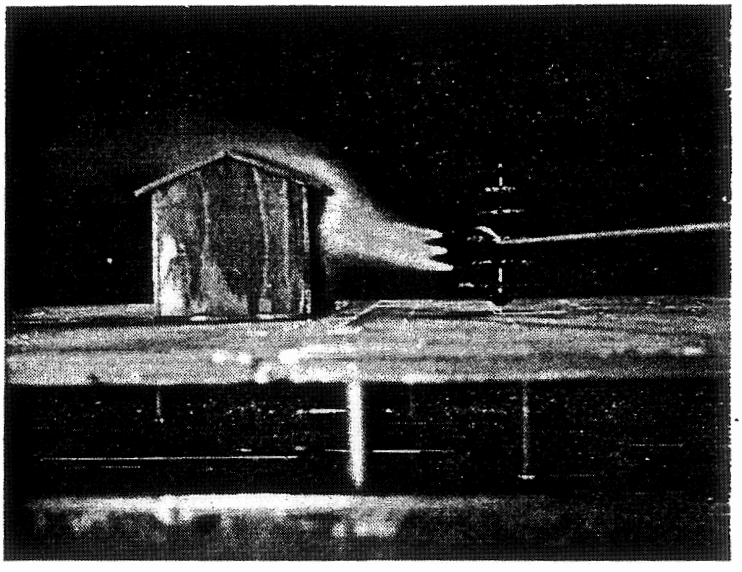

Figure 2: Sample Smoke-Tunnel Test Showing Model House, Tree, Smoke Rake and Stream

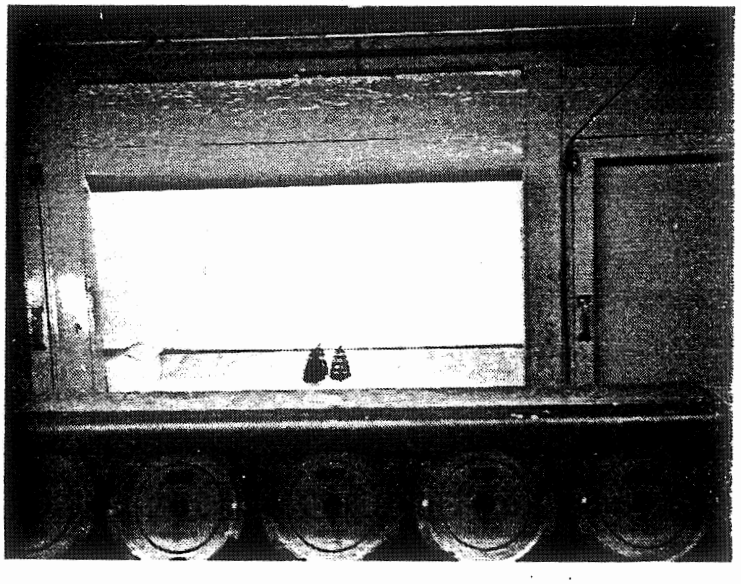

Figure 3: View of Force Tunnel Testing Area

2.2 FORCE TUNNEL TESTS

The force tunnel tests were so called because they were conducted in the Princeton University Subsonic Laboratory 3.5 x 5' "Force" wind tunnel. This tunnel has a contraction ratio of 5 and a maximum windspeed of over 100 mph. To save wear and tear on the tree models, the tests were conducted at 65 mph(6). This tunnel is particularly suited to the simulation of planetary boundary layer flow due its large tunnel-to-model-streamwise-cross-sectional area. This means that the air is compressed relatively little in passing around the model so the velocity in the model vicinity is not appreciably increased because of partial reduction of the tunnel cross-sectional area. A picture of the tunnel testing area with models in place as seen through the operators window is shown in Figure 3. Windflow is from right to left.

A 4 foot wide, 3/4" thick plywood ground plane ran the length of the test area. The house model was mounted in the downstream test section area. It was constructed of 1/4" plywood, and was a 1/48th scale model of a simple two-story house with a gabled roof. A closeup of the house as mounted on the ground plane may be seen in Figure 4.

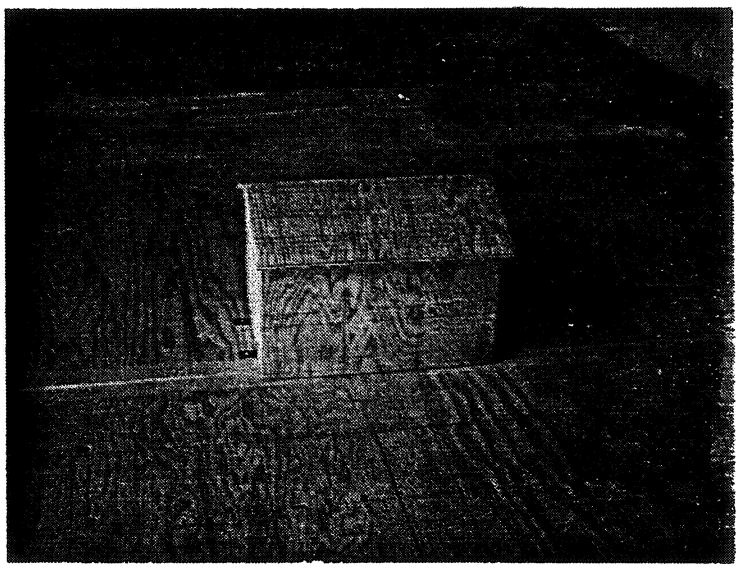

Figure 4: Closeup of Model House Mounted on Ground Plane

---

6. For velocity similitude analysis, see section on Similitude.

The house was fitted with 66 pressure taps mounted in the walls and roof as shown in Figure 5, where each dot represents a pressure tap with associated surface area. The dimensions of the house model are also shown. The air tubes connected to the pressure taps passed to the exterior of the wind tunnel via a hole in the ground plane and tunnel floor beneath the house mounting position. The lines are connected to a manometer board adjacent to the wind tunnel.

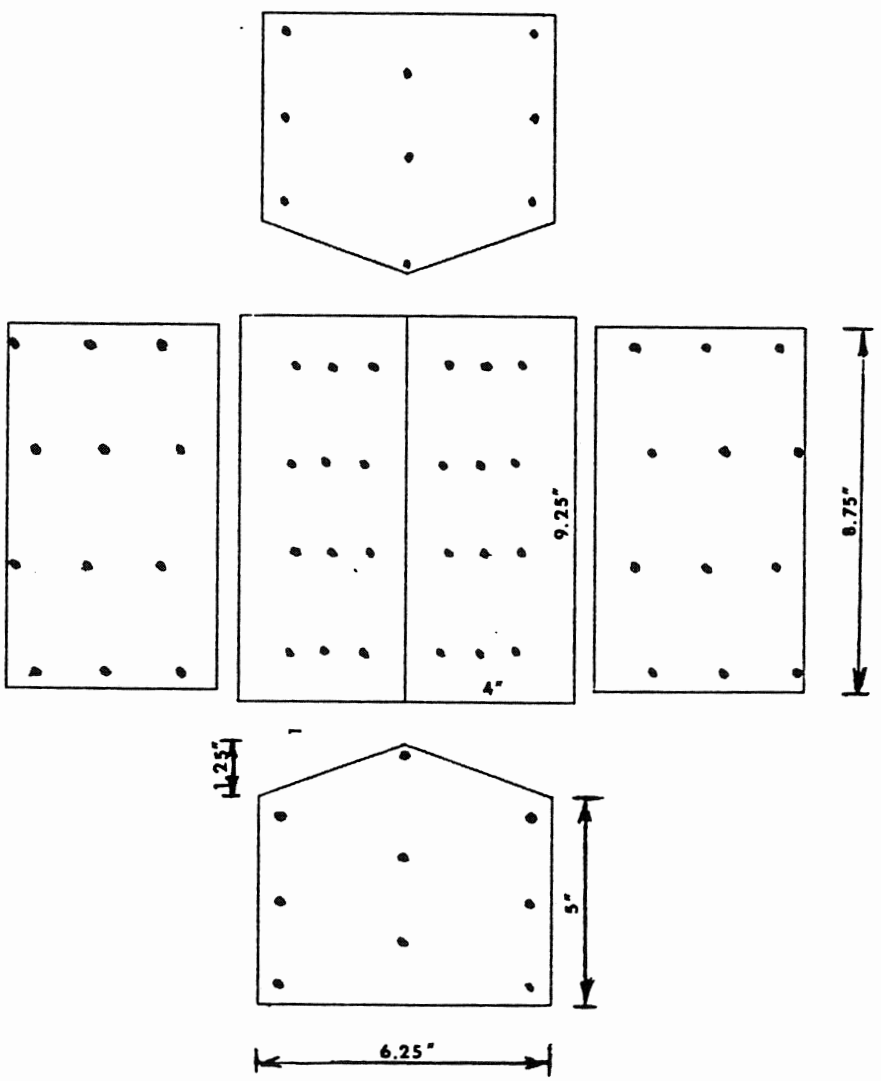

Figure 5: Plan View of House Surfaces Showing Location of Pressure Taps

Tunnel dynamic pressure was measured by a Pitot tube mounted 20 model feet(7) above the ground plane, 280 mf upstream of the house, and 70 mf off tunnel center. A reference static pressure as measured by a tap located in the test area side wall 40 mf above the ground plane and 120 mf laterally displaced from the house. Tunnel pressures were also represented on the manometer board. Figure 6 shows a sample testing setup with the locations of the reference tap and Pitot tube.

In order to facilitate rapid collection of the many manometer board readings, a general-purpose photographic collection system was devised. A high resolution Graflex portrait camera was fitted with a Polaroid film back. This camera was positioned so that the film plane was parallel with the plane of the manometer tubes, as shown in Figure 7. In running a test on a given configuration, when the manometer columns were stabilized with the windtunnel running at

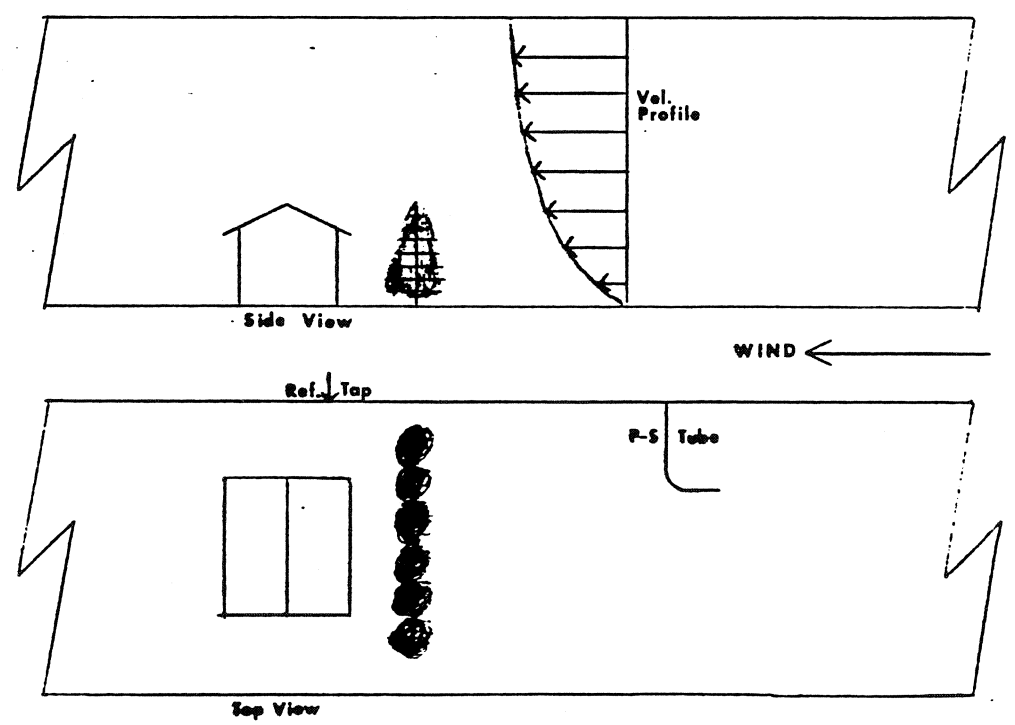

Figure 6: Sample Test Setup Showing Locations of Pitot Tube and Reference Tap

7. 1 model foot [mf] = 1/4 inch, or 1 foot scaled by 1/48th.

simultaneously on Polaroid type 47 film. A sample test results photograph is shown in Figure 8.

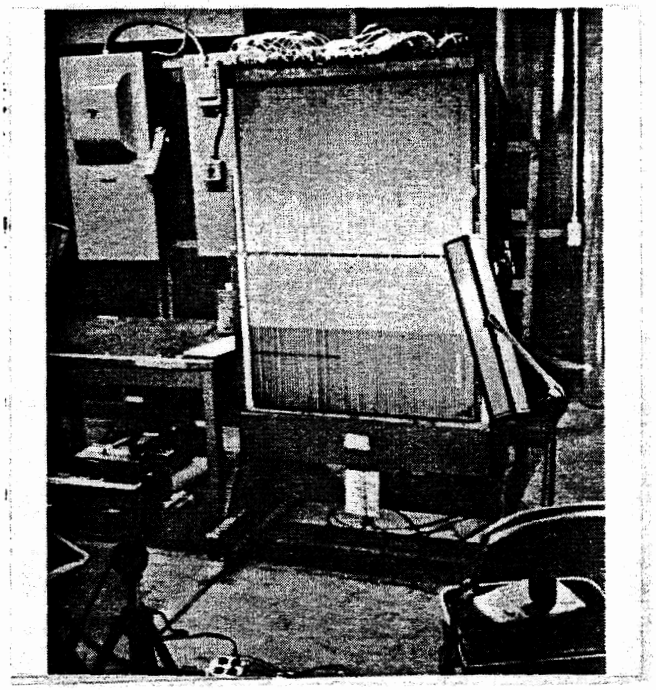

Figure 7: Manometer Board and Recording Setup

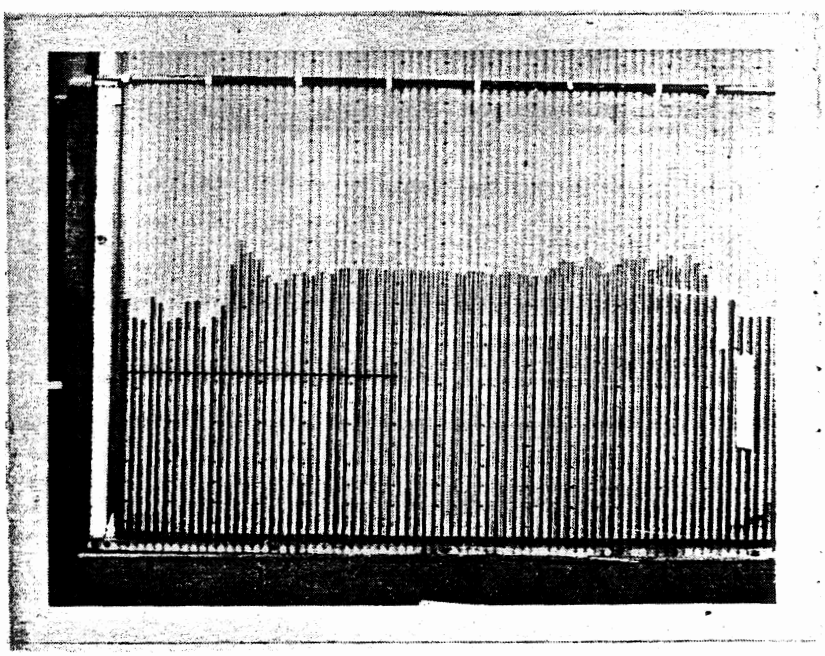

Figure 8: Sample Test Results Photograph

These photographs were "read" using a Tektronix 4954 Graphics Tablet system. Using an ordinary high intensity opaque projector, an image of each test photograph was projected onto the graphics tablet, a large plane surface equipped with a sort of radar system for the finding of points on the plane. Using a special cursor that is interfaced electronically with the graphics tablet, the user points out on the surface of the tablet a location to be marked, and presses the "mark" button on the cursor. The point is now said to be digitized. The tablet electronics determine the x,y coordinates of the point, and send them through a time sharing terminal to a computer. A picture of the graphics tablet system in use, here collecting the locations of bus stops in a large city, is shown in Figure 9.

By digitizing a series of reference points to aid in calculating scale and orientation, and then the tops of the manometer alcohol columns, it is possible to calculate the relative heights of these columns and hence the relative pressures. The probable error(8) introduced due to the use of this data processing technique was found to be less than 1%.

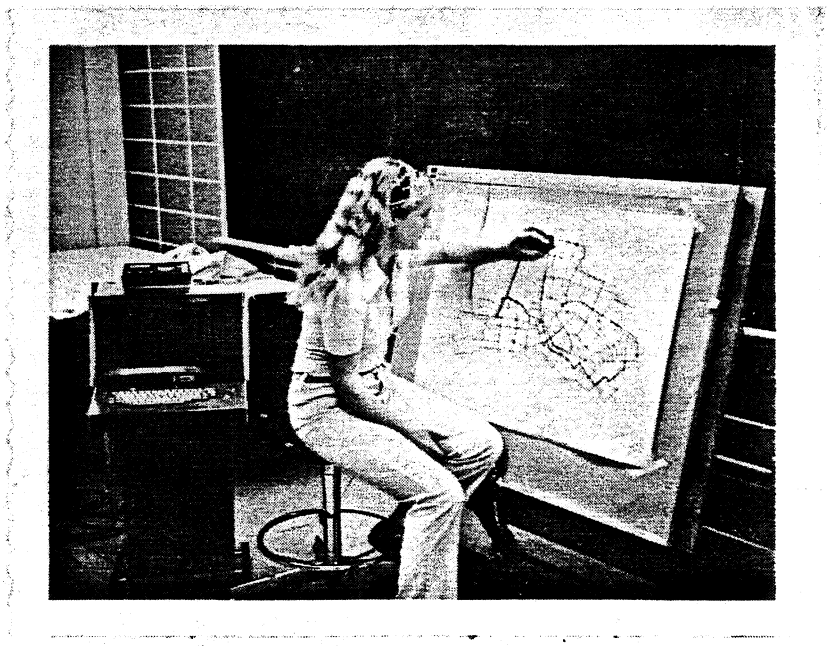

Figure 9: Graphics Tablet System in Use

---

8. the defined statistical index.

From these data three types of results were calculated using the method of Mattingly and Peters(9). The pressure on the house interior, presumed to be uniform throughout, is calculated as a weighted average of the exterior wall pressures, using the external wall areas associated with each tap as weighting factors. That is:

$$P_{int} = \frac{\sum_{k=1}^{\#taps} A_k P_k}{\sum_{k=1}^{\#taps} A_k}$$

where A(k) is the house surface area associated with pressure tap k, and p(k) is the pressure of that tap, minus tunnel reference static pressure.

The pressure coefficient with respect to the interior pressure for each tap is given by:

$$Cpi_k = \frac{P_k - P_{int}}{P_{dyn}}$$

where p(dyn) is the dynamic pressure as determined by the Pitot tube. These pressure coefficients are plotted against their house surface location for each test in an auxiliary reference given below(10). This document will be referred to in this report as the CTPD. The method for interpreting the plots in the CTPD and a sample data page for test 1 are given in Appendix 3.

---

9. Mattingly and Peters, pp. 24-29. The only significant extension is that the house surface was divided up into 66 subsurfaces, 1 subsurface per pressure tap, instead of considering each wall as one surface and averaging tap pressures for that wall. Each area of surface of the house that actually communicated through a simple wall to the interior (i. e. excluding the roof overhangs) was assigned to the nearest pressure tap on the same surface.

10. Buckley, C. E., "A Catalog of Test Pressure Coefficient Distributions for Use With Optimum Use of Coniferous Trees Study", Center for Environmental Studies Draft Report, January 1978

Lastly, the AI parameter is given by:

$$AI = \frac{\sum_{k=1}^{M} \langle Cpi_k \rangle^{+} A_k}{A_{char}}$$

That is, AI is a weighted summation over all M taps where M is the number of taps whose Cpi is positive. A(char) is a characteristic area of the model, here chosen to be the area of the front wall.

The AI parameter is a dimensionless index of the propensity of a given model house to be subject to wind-induced air infiltration, and is controlled by the distribution of the approaching wind. If similitude requirements are met(11), AI should be independent of windspeed. AI should not be confused with actual air infiltration, which is caused by wind and the stack effect, and is given in units of volume flow, such as cubic feet per hour.

AI parameters for each test run are listed in Appendix 1.

2.3 SIMILITUDE

The principles of modelling similitude were carefully adhered to in preparing the force tunnel tests. All practical similarity requirements as outlined by Sadeh(12) were met.

Geometric similarity was attained through careful scale modelling of house and tree elements. In accordance with tree similarity requirements as described by R. N. Meroney(13), drag characteristics were also matched between model and full-scale by varying the wrapping density of the trees as described in the section on trees, below.

---

11. See section on similitude, below.

12. Sadeh, Willy Z., "Weather-Climate Modeling for Real-Time Applications in Agriculture and Forest Meteorology", Preprints from Thirteenth Conference on Agriculture and Forest Meteorology, West Lafayette, Indiana, April 4-6, 1977

13. Meroney, R. N., "Characteristics of Wind and Turbulence in and above Model Forests", Journal of Applied Meteorology, V. 7, p. 780

Kinematic similarity was achieved through matching the scaled velocity profiles and hence roughness heights of upstream terrain between prototype and model. Figure 10(14) shows a plot of the two profiles non-dimensionalized by properly scaled reference heights(15).

Dynamic similarity is met easily. Minimum Rossby and Reynolds number requirements were met. The Reynolds number of the full-scale situation is 2,170,000. The corresponding modeling Reynolds number is 300,000. Both are greater than 100,000, thereby satisfying the Sadeh criterion.

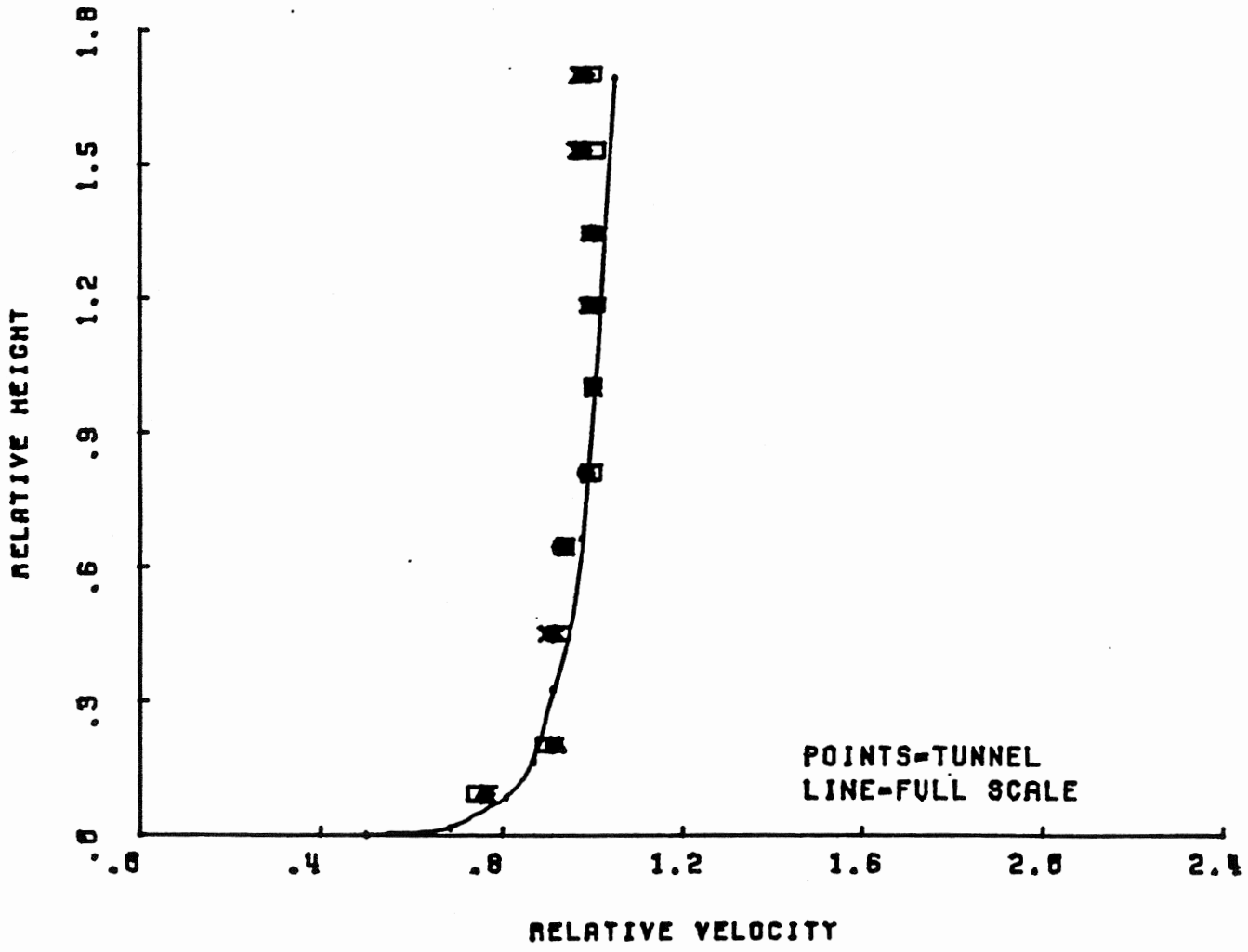

Figure 10: Full Scale and Tunnel Boundary Layers

---

14. full scale data provided by. and used with permission of Dr. G. E. Mattingly

15. i. e. the model reference height is 1/48th of the full-scale reference height.

Thermal similarity is met easily on the house exterior where, due to the high flow rate, low stratification nature of the wind conditions, both model and full-scale Richardson numbers are essentially zero.

2.4 TREES

The modelling of trees in this study to correctly simulate full-scale wake and drag coefficients was based on the assumption that the majority of the drag of a tree is caused by its foliage and small branchwork, which is concentrated around the outer part of the tree crown. This is considered a good approximation since as inner foliage is shadowed by outer foliage as the tree grows, it atrophies through lack of light (intolerance). This tree modelling approach was used by Fraser(16).

A survey of spruce and cedar trees in the Princeton area was made, and the silhouettes of representative mature, open-grown trees were recorded. These silhouettes are given in Appendix 2. Spruce and cedar trees were selected on the basis of their high foliage density, even foliage distribution, and high tolerance.

The tree shapes were scaled by 1/48th and to the model tree height desired, and these shapes were then transferred onto stiff cards. The tree areas were cut out of these cards. Depending on the trunk thickness needed, either stiff steel wire or aluminum 1/4 inch round stock was used as a tree trunk, and on this trunk were placed wire mesh platters spaced one inch apart. The radii of these platters were such that when mounted on the trunk, the platters fit through the silhouette of the tree shape card with a sixteenth inch clearance on either side. A platter separation of one inch was chosen because it yielded a drag coefficient of approximately .18, which is small compared to total tree drag.

Knitting yarn was wrapped vertically around the tree so that the yarn coverage per unit area was constant over the entire crown surface. Variation of the yarn wrapping density determined the drag coefficient of the tree. The drag coefficient of a particular wrapping density was determined experimentally using a platform balance in the wind-tunnel. A detailed drawing of a tree mounted on the platform balance is shown in Figure 11. A photograph of a tree being checked for shape fidelity is shown in Figure 12.

---

16. Fraser, A. I., and Walshe, D. O., "Wind Tunnel Tests on a Model Forest", National Physical Laboratory (U. K.) Aero Report /1078, October 1973, p. 3

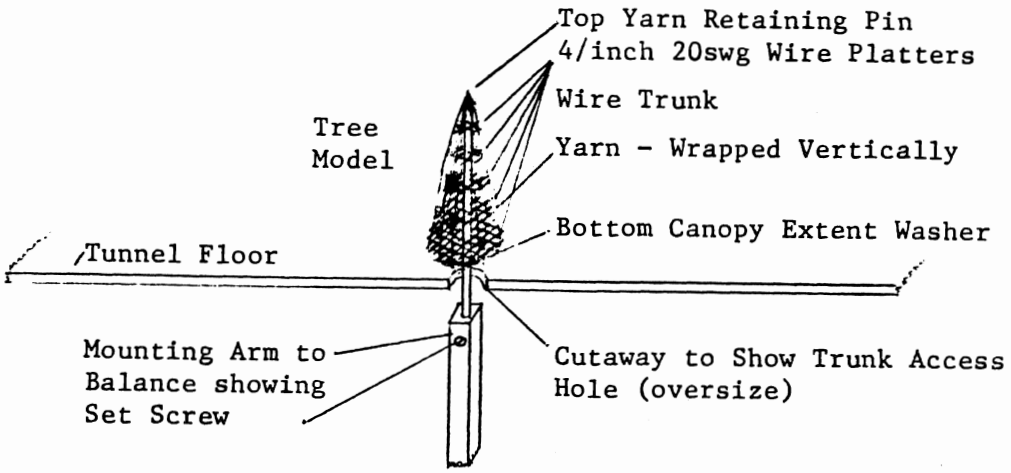

Figure 11: Detailed Drawing of Tree Mounted on Force Tunnel Platform Balance to Determine Drag Coefficient

It was decided on the basis of shape that the trees best suited to windbreak use of the ones surveyed were the Colorado spruce (Picea pungens Engelm.), Norway spruce (Picea abies L.), and Atlantic white cedar (Chamaecyparis thyoides L.). These all have approximately the same shape, and were thus represented in the study by the Norway spruce shape. For studies of the effects of tree underpruning, the shape of an eastern red cedar (Juniperus virginiana L.) was used.

Most tests were conducted with trees 25 model feet tall, as this was very near the height of the house. However, trees of other heights were constructed as appropriate. The nominal drag coefficient of the trees was chosen to be .58 after the full-scale wirdtunnel studies of spruce trees conducted by Raymer(17), but trees of other drag coefficients were constructed as needed. A picture of the battery of model trees used in the force tunnel studies is shown in Figure 13.

---

17. Raymer, W. G., "Wind Resistance of Conifers", National Physical Laboratory (U. K.), Aero Report /1008, April 1962, Table 1.

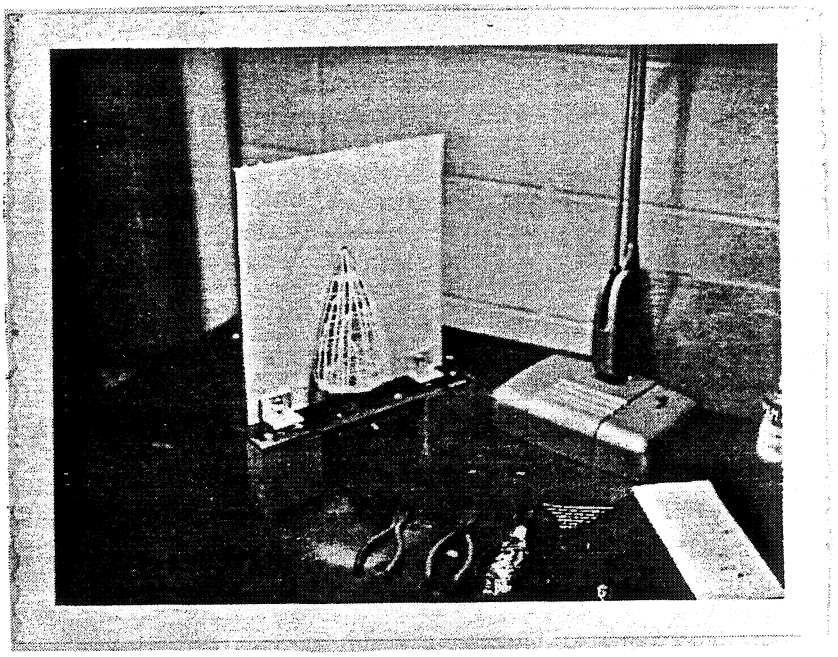

Figure 12: Model Tree Being Checked for Fidelity against Original Surveyed Shape

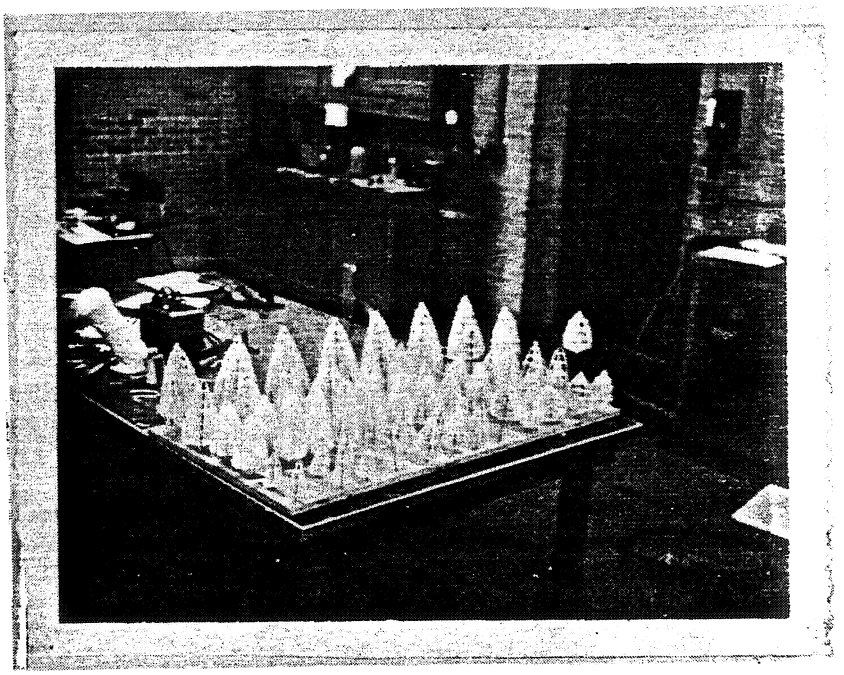

Figure 13: Model Trees Used in Tests Shown in Lab Storage Racks

3. RESULTS

In view of the large number of tree and house configurations that could conceivably be tested in search of an optimum configuration for wind protection, series of tests were devised to determine the effects of variation of one particular parameter in a house/tree configuration, by varying this one parameter and holding all others constant. Those series of tests which were performed are described below, along with the results of those tests. The numbers following the name of each series refer to the test runs from which the results were drawn. They are included as a cross reference feature in case the reader desires to examine the actual pressure coefficient distributions in the CTPD, or the AI values listed by test in Appendix 1.

3.1 HOUSE ALONE SERIES - (1,2,3,4,5,6)

The house was tested by itself in the windtunnel at three angles to provide control readings for comparison with tree/house readings. Also, the independence of the AI parameter on tunnel windspeed was tested.

Air striking a house stagnates on its windward wall, and forms a high pressure vortex there as shown by the dense cloud of smoke in Figure 14. Windflow is from right to left. The air must bleed away to satisfy continuity, and it does so, with a greater propensity to flow around the side walls than over the windward roof, due to the presence of the eaves. This is evidenced by Figure 15. Also, air pressure on the windward wall is higher at the center than at the sides due to the Bernoulli effect of the air rushing around the corners(18).

The behavior of air flowing around the side walls of the house is demonstrated by the two-dimensional smoke-flow pattern shown in Figure 16. The important factor here is that the flow is separated from the side walls at the wall corners, creating an area of low pressure on the side walls.

---

18. CTPD, test 1

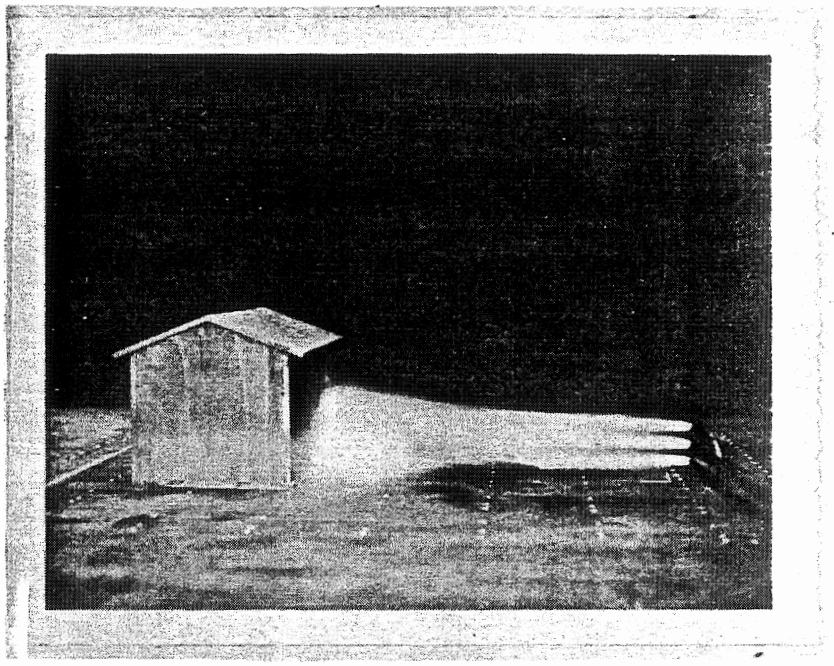

Figure 14: Stagnation Zone on Windward Wall of House

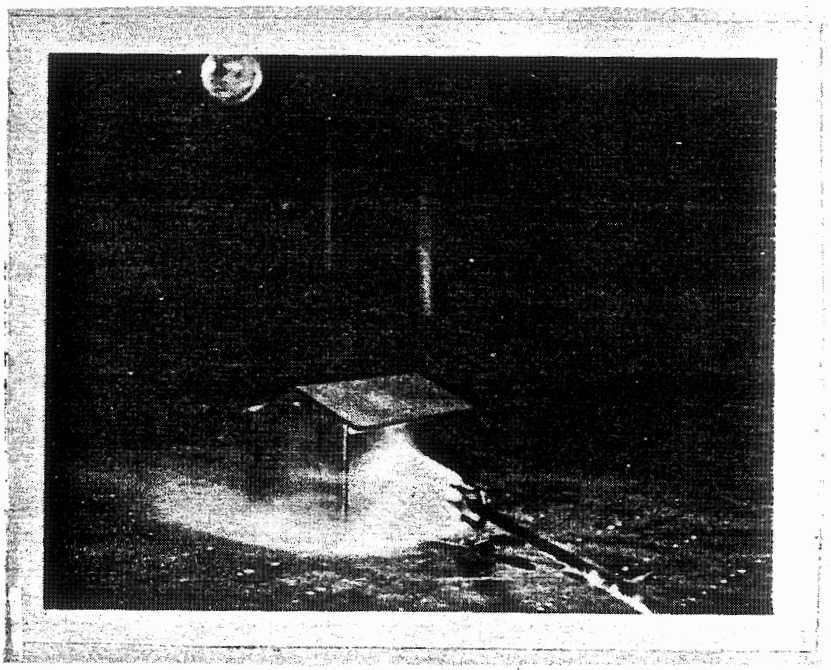

Figure 15: Dispersal of Air from Front Wall

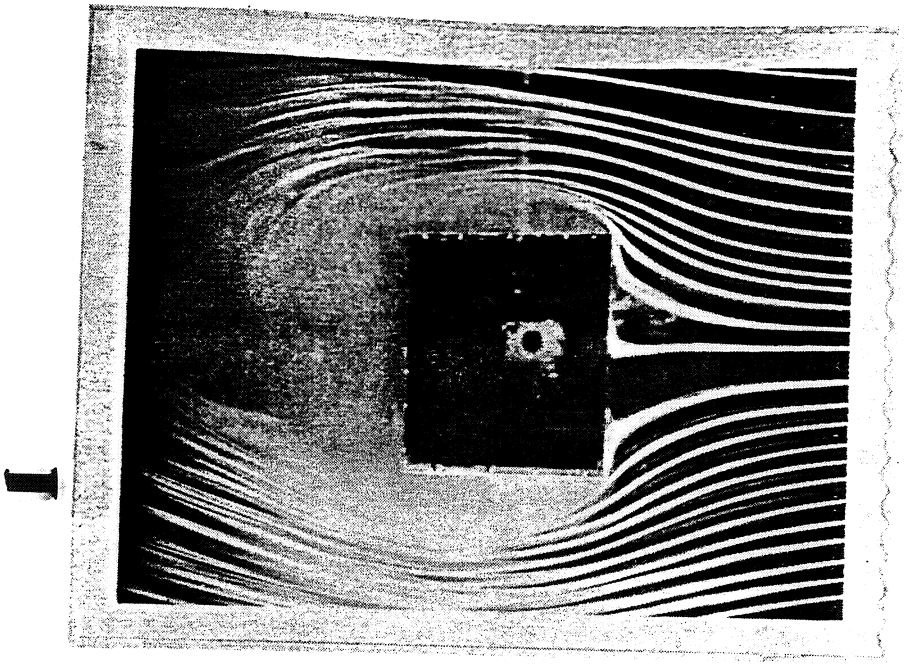

Figure 16: Top View of Flow around Side Walls of House

Low pressure air circulates within the cavity, flowing upstream along the side wall. This can be seen on the upper side wall in Figure 16, and even more so in Figure 17, where ambient windflow is from right to left, so the air is apparently flowing upstream. The air flowing upstream is sheared off at the upstream side wall corner by air coming off the front wall, and is carried downstream.

Figure 17: Manifestation of Slow Pressure Vortex on Side Wall of House

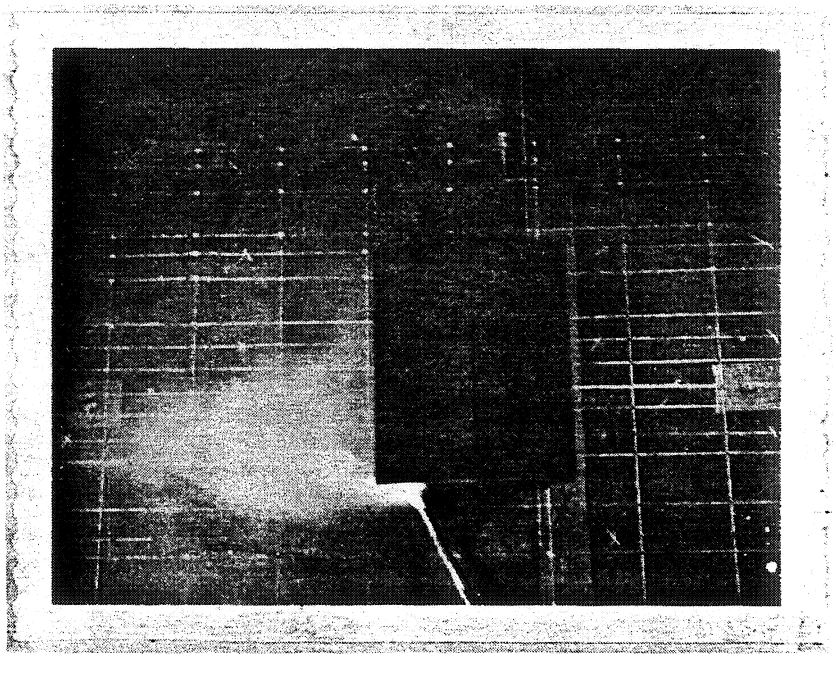

Figure 18: Air Supply to Downstream Wall

The streamlines that separate from the side walls of the house in Figure 16 continue in a cohesive manner downstream. This shows that the air flowing across the downstream (leeward) wall is supplied from the low pressure regions adjacent to the side walls. This is shown in Figure 18, a view of the downstream part of the house from above, where air off the side walls curls into flow across the downstream wall. Finally, the air on the downstream wall migrates up over the downstream eaves to the downsream roof where it is sheared away at the rooftree by airflow over the top of the house, as shown in Figure 19. This airflow separated from the roof of the house at the rooftree(19).

Figure 19: Migration of Air from Downstream Wall to Downstream Roof and Away

---

19. The rooftree is the uppermost ridge of a pointed roof.

When the calculations as described above are carried out, it is found that the areas of greatest interior-exterior pressure differential are located in the upstream wall where pressure is highly positive (greater on the outside than on the inside), and on the upstream roof and upstream parts of the side walls, where pressures are highly negative (greater inside than out). The pressure differentials on the downstream walls, roof, and downstream parts of the side walls are small in comparison to the upstream values, and do not contribute greatly to wind-induced air infiltration.

Hence it is concluded that air in- and exfiltration occur primarily through the windward surfaces of a house. This is seen in the pressure coefficient plot found in Appendix 3.

AI is increased somewhat when the house is angled at 45 degrees with respect to the windflow(20), since the downstream roof panel is subject to some high-speed flowby of air just as is the upstream roof panel(21). In the 0 degree or normal case, the downstream roof was protected from this flow, which tends to cause exfiltration through the surface, by the upstream presence of the rooftree discontinuity. The rooftree caused the flow to separate in the 0 degree case, as shown in Figure 19, but not in the 45 degree case.

With the house angled at 90 degrees, the same absence of rooftree protection brings high-speed flow along the roof surface and therefore greater air exfiltration through the roof. However, the reduced frontal area of the house positioned so that its smaller walls lie windward and leeward tends to offset the increase in AI through the roof. Although there is some flow off the roof onto the leeward wall, as shown in Figure 20, the leeward wall pressure remains very close to house interior pressure.

---

20. At 0 degrees, the front wall plane, rear wall plane, and rooftree line are perpendicular to the direction of windflow.

21. CTPD, test 2

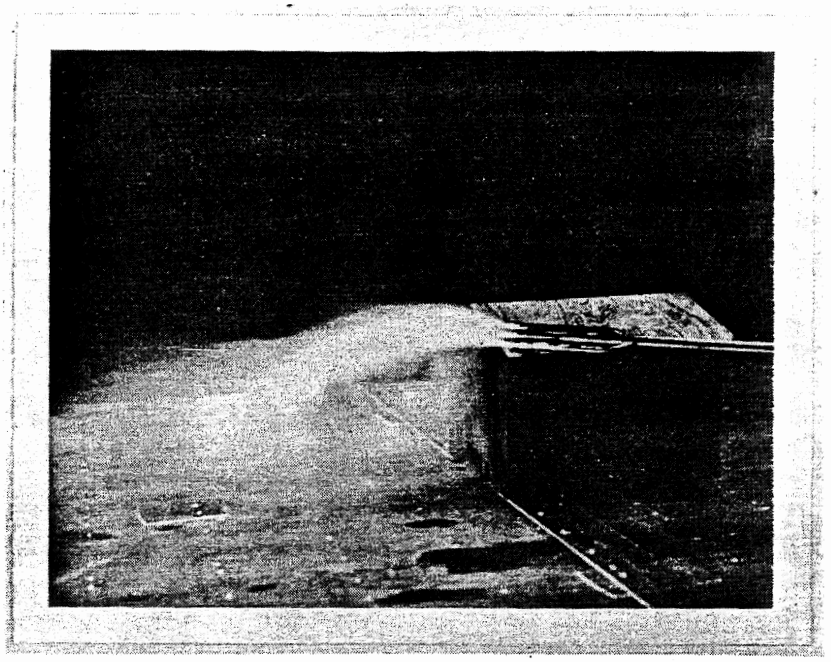

Figure 20: Flow off Roof into Leeward Area with House at 90 Degrees

The location of the roof panels in the tests pertaining to the above discussion can be seen in the plan views of the house alone tests conducted at the three angles as shown in Figure 21, along with the AI values calculated from each test. The house is at 0 degrees, or facing normally, in the left hand frame. The line across the top of the house is the roofline. The angle of the house with respect to the wind has very little bearing on AI; the AI's for the three angles did not vary by more than 15% of the smallest value.

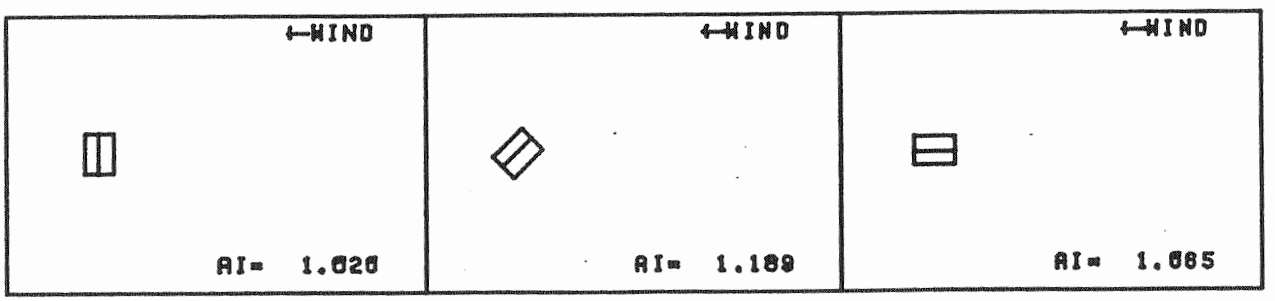

Figure 21: Plan Views of House Alone Tests at 0, 45, 90 Degrees With Resulting AI's

The three "house alone" test AI's measured at various windspeeds show only a very small inverse dependence if any at all on the tunnel windspeed. The standard deviation from the mean (assuming random distribution) is less than 1%, and the AI values ranged over 4.5% of their mean for a 50 mph windspeed variation. Therefore, it was concluded that variations in the AI parameter are indicative of variations in wind-induced air infiltration regardless of the ambient windspeed encountered, over the windspeed range one would expect in a full-scale situation.

3.2 SINGLE TREE SERIES - (7 THROUGH 24)

A single tree was placed directly upstream of the house at varying distances, and at a constant distance upstream while varying lateral displacements from directly upstream, to determine the sheltering effects of a single tree for use in special applications.

These tests show quite well the mechanism whereby trees provide wind shelter. Figure 22a shows a stream of smoke released in the smoke tunnel with nothing in its path. Figure 22b shows what happens when, without moving the smoke rake, a spruce tree with a standard drag coefficient of .58 is placed in its path. The smoke stream is not noticeably deflected, and flow immediately downstream of the tree appears the same. By the time the smoke is about 45 model feet downstream(22), it is moving visibly slower. Small scale, side-to-side turbulent motion of the air is greatly increased. This is important. These tests indicate that trees do not afford protection so much by deflecting windflow, but rather by allowing flow to pass through the tree crown. In the crown the air flow is randomized through foliage friction, so that as flow passes further downstream, its turbulence and random velocity increase, with a resulting decrease in net flow velocity. This results in reduced air pressure when the flow is stagnated on downstream objects such as houses.

---

22. Each row of dots represents 15 model feet.

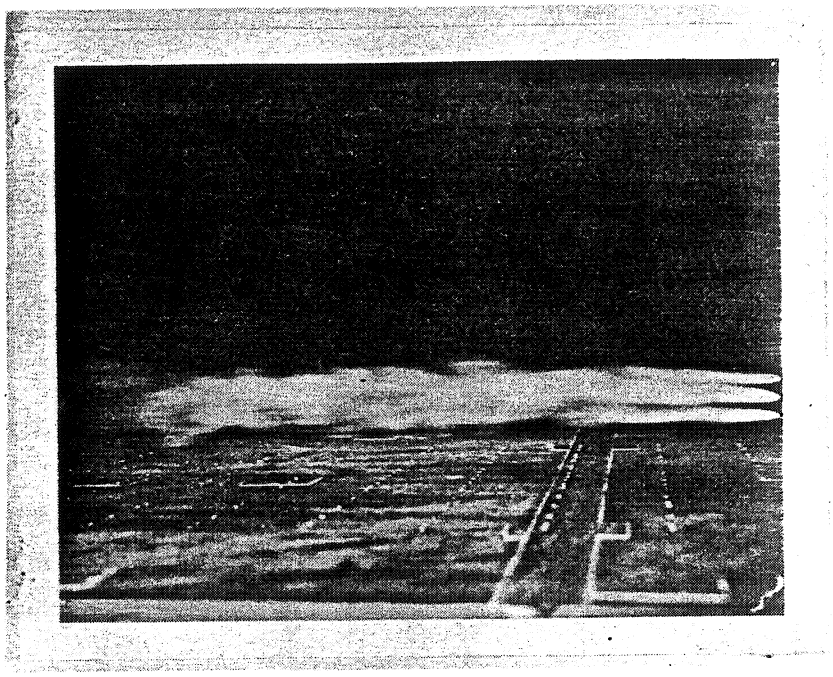

(a) - Smokestream with no Tree

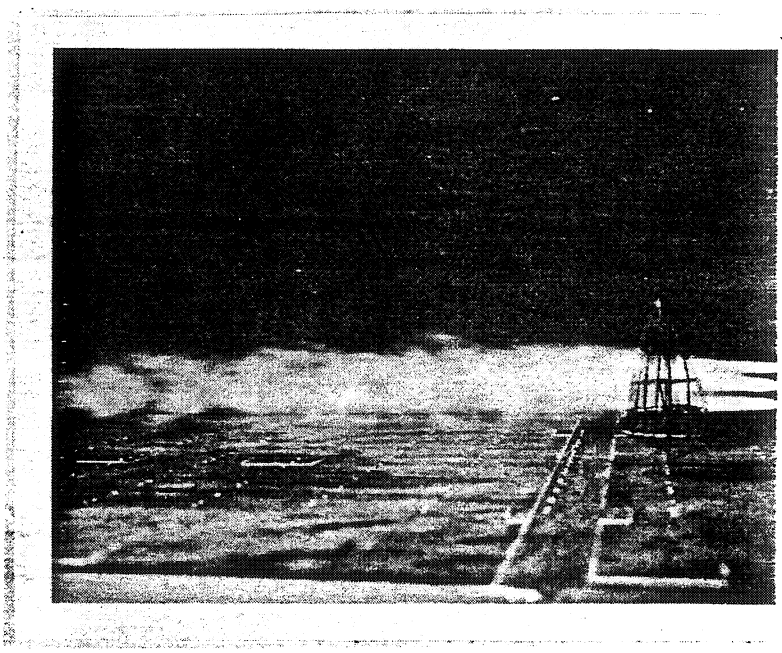

(b) - Smckestream with Normal Drag Tree

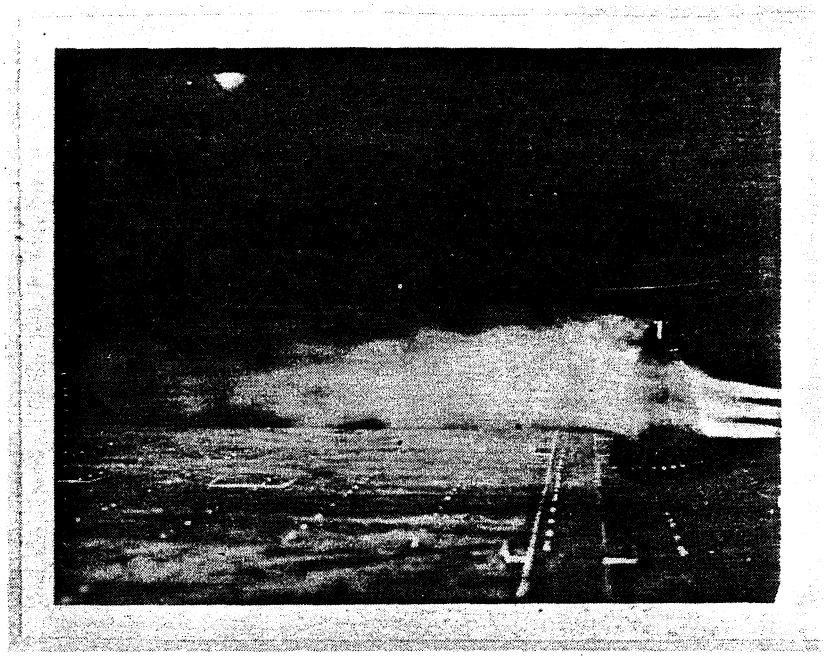

(c) - Smckestream with High Drag Tree

Figure 22: Mechanism of Tree Wind Sheltering

A single tree was constructed with an unreasonably high drag ccefficient of .92 and placed in the smokestream described abcve. The result is shown in Figure 22c.

Here there is some flow deflection such as would be experienced with a bluff body or a dense row of trees such as those described in the hedgerow tests below. A single tree with such a drag ccefficient will not normally be found in nature.

Figure 23 shows a plot of AI parameter over distance upstream from the windward house wall for a single tree of normal drag. The range of maximum effect is 45-120 mf. The maximum AI reduction is 30% at 60 mf. With the tree closer to the house, the protection afforded is less since the turbulence of the air flowing out cf the tree has not been fully developed. Further away than 120 mf, the effectiveness of the tree is reduced as air flowing through the tree remixes with air flowing around the tree before it reaches the house. With the windbreak located far from the house, the shapes of the pressure coefficient distributions appear very similar to those of the house alone. At distances of low AI, air infiltration is reduced primarily due to a localized reduction cf pressure on the windward wall directly downstream cf the tree, with accompanying reduction of the pressure drawdown on the upstream portions of the roof and side walls(23).

---

23. CTPD, tests 9-13

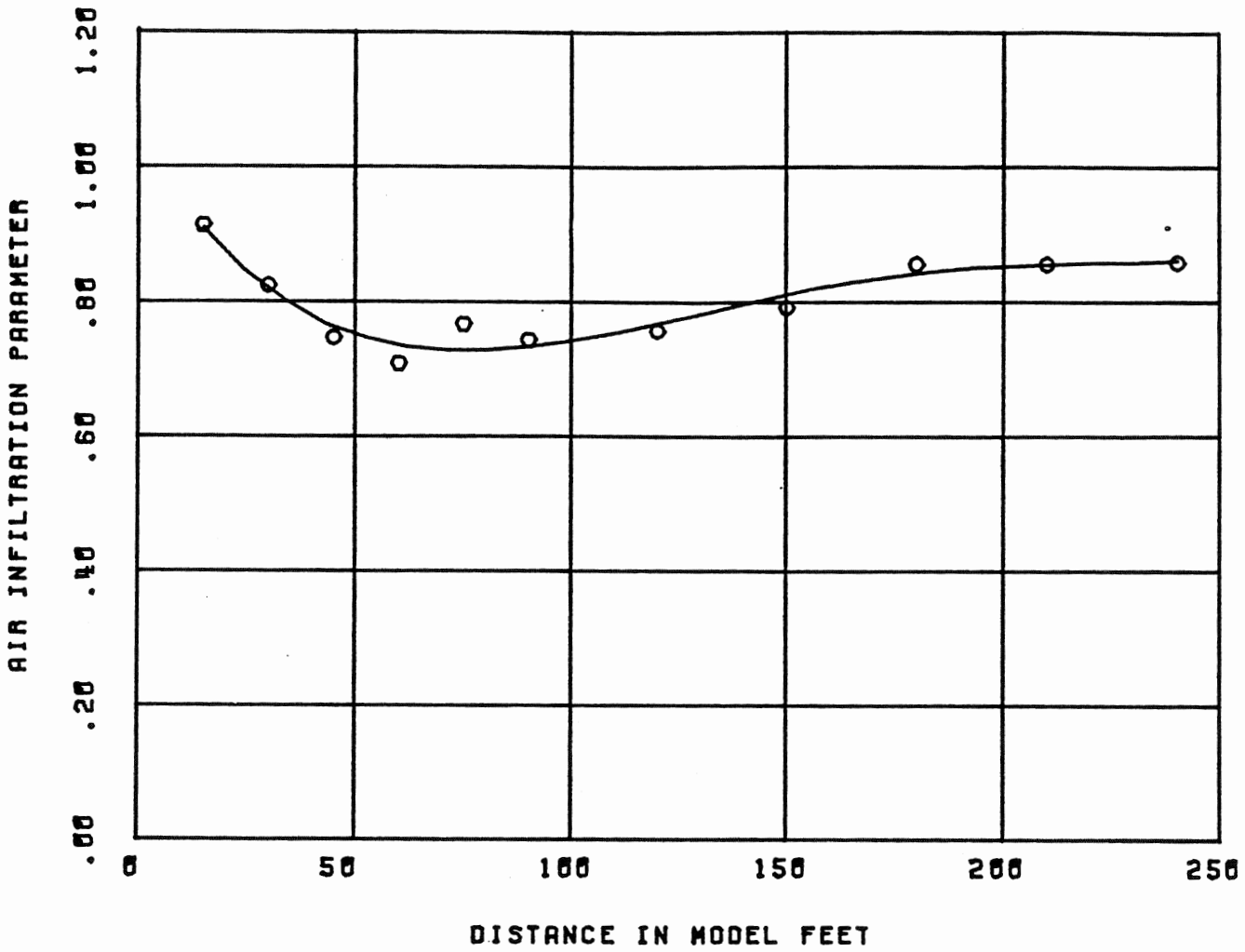

Figure 23: Plot of Single Tree AI over Distance

Figure 24 plots AI parameter for a single tree as it is maintained at a constant upstream distance from the house, and displaced laterally(24). The curve shows simply that a single tree influences only what is directly downstream of it. When the tree is laterally displaced only 20 mf from directly upstream, it is as if no tree were protecting the house at all. The front wall of the house facing normally is 35 mf wide. Half of this is 17.5 mf, so at 20 mf of lateral displacement, the tree is just barely out of the windflow corridor in which the house lies.

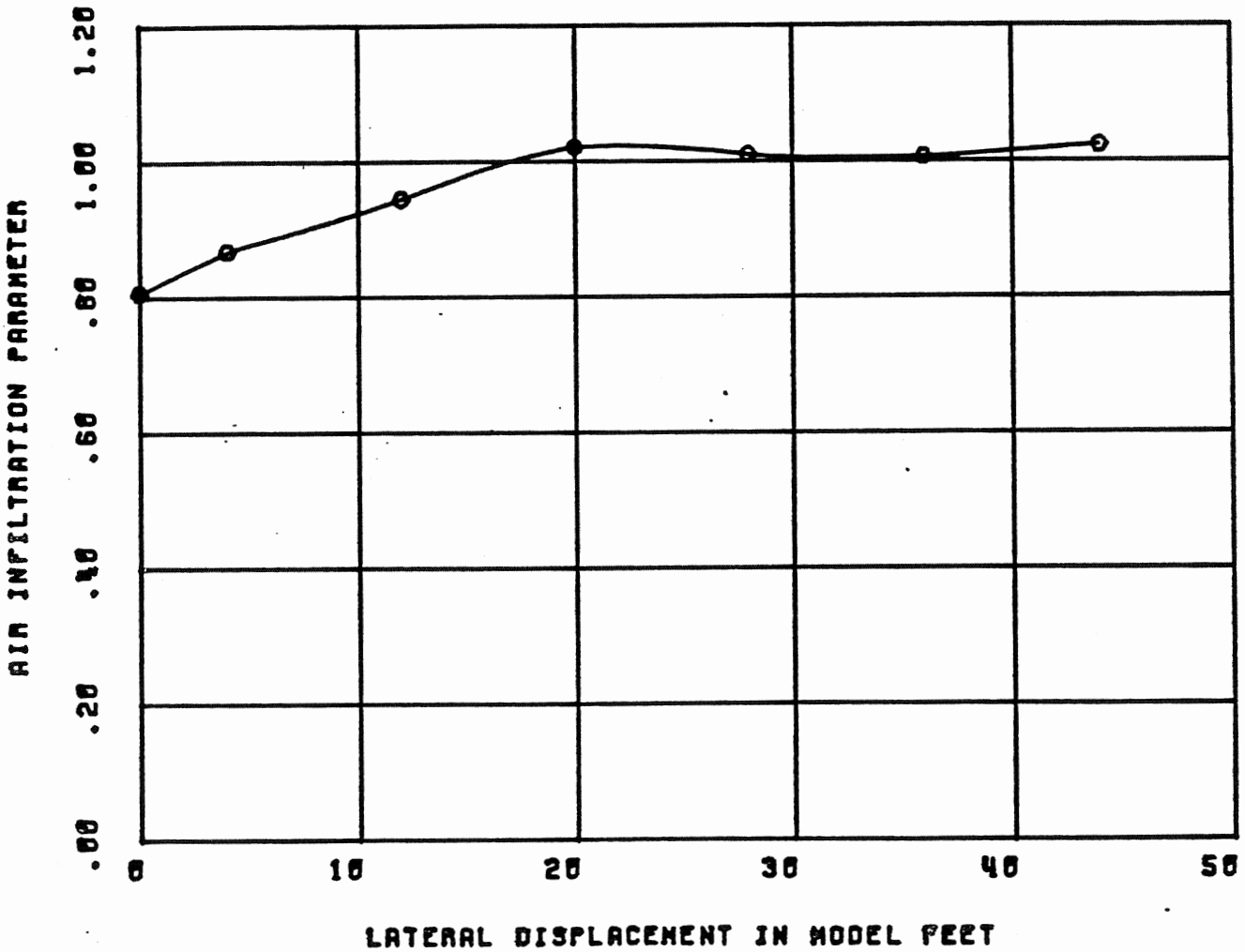

Figure 24: Plot of Single Tree AI over Lateral Displacement

---

24. CTPD, tests 18-24

3.3 DISTANCE AND REPEATABILITY SERIES - (25 THROUGH 41)

Models of a row of open grown trees and a row of trees grown together in a hedgerow were tested at various distances upstream of the house to determine the change in effect of these rows with house-tree distance, and to compare the effectiveness of a traditional, closed-style windbreak with the more economical open row. Also, the open row tests were run repeatedly on separate days with different trees constructed in the same manner to determine the repeatability of the experimental methods used.

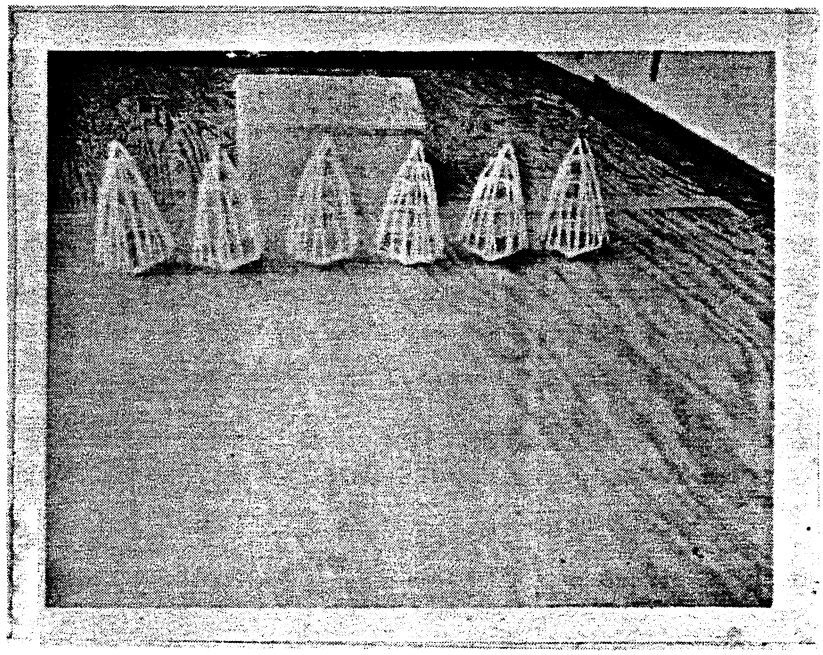

Figure 25: Picture of Open Row Configuration

In the open row tests, whose configuration is pictured in Figure 25, the shapes of the pressure coefficient distributions resemble the shape of those for the house alone, although the pressure drops across the surfaces are not as great(25). This is reasonable when one considers that in the open row tests there is a uniform barrier upstream of the house, as opposed to the point barrier characteristic of the single tree.

25. CTPD, tests 25-35 as compared with test 1

Figure 26 shows a plot of the AI of tests of the open row positioned at various distances upstream of the house. The very same reduced effectiveness at near distances that was seen with the single tree (Figure 23) is present here, but the reduction at far distances takes effect more slowly and to a lesser extent as the trees move out. This is simply due to the fact that more directed kinetic energy in the airflow has been converted to random turbulent energy. Since the quantity of unaffected air flowing adjacent to the windbreak path of effectiveness is not increased, it takes longer for this free flowing air to remix with air which flowed through the windbreak.

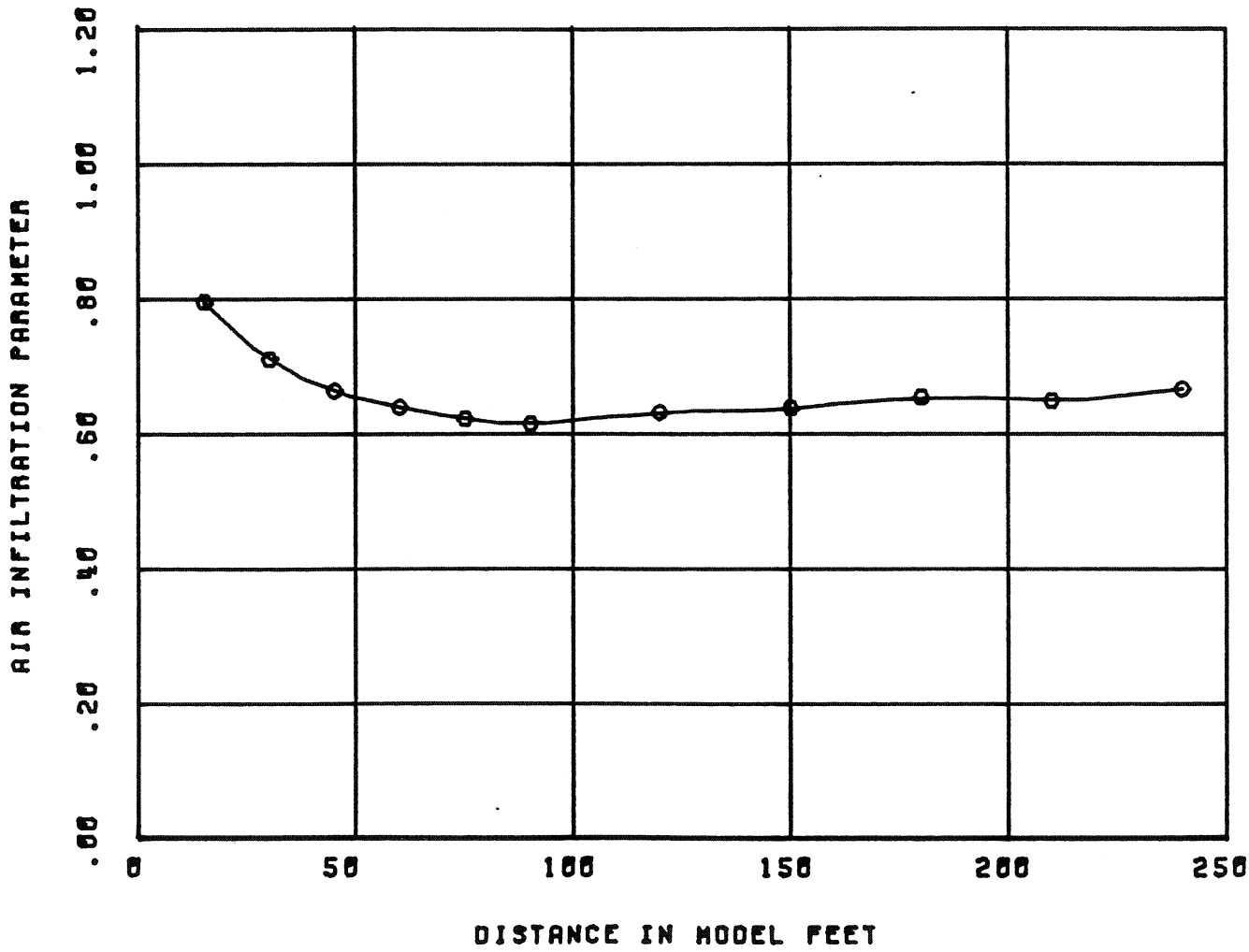

Figure 26: Plot of Open Row AI over Distance

The reduction of AI due to the open row at the distance of maximum influence of 75-110 mf is attributable mainly to reductions in pressure drops across the windward wall, and windward ends of the side walls and windward roof(26). The maximum AI reduction acheived is 40%(27) at 90 mf. This is only a small improvement over the single tree, but inasmuch as the open row is effective on winds approaching from a range of directions, such a comparison is unfair. The comparison does highlight the fact that the amount of windbreak protection a house receives is dependent only on the trees directly upstream of the house when the wind is blowing.

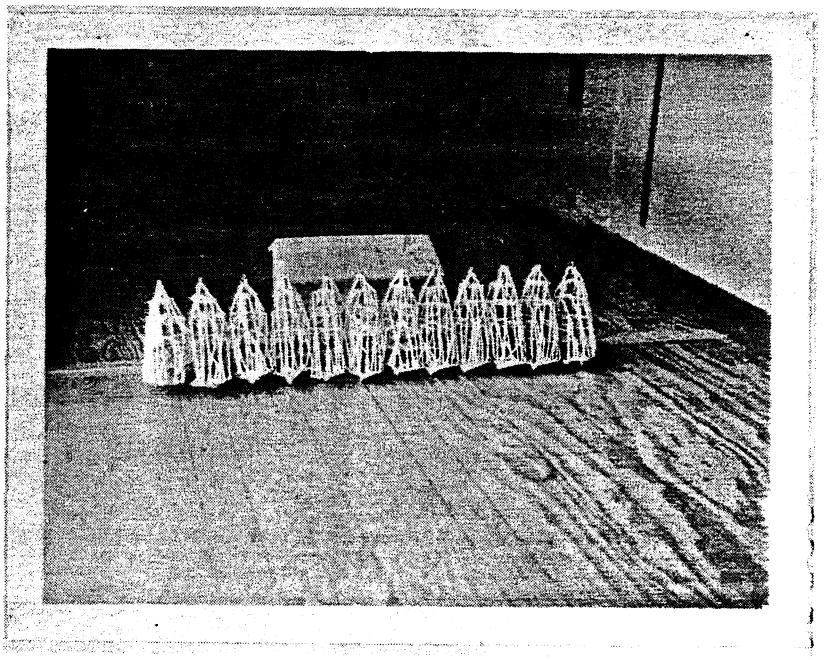

Figure 27: Picture of Hedgerow Configuration

---

26. CTPD, tests 29-30

27. Percent AI reduction is defined to be the percentage of unprotected house AI (for the house oriented at a particular angle) eliminated by the placement of a given tree configuration.

Figure 27 shows the hedgerow configuration, and Figure 28. plots the AI of a hedgerow over house/tree distance. The salient feature of a hedgerow (as compared to an open row, in which there is space between trees) is that the crowns of the trees comprising it have grown together. With a hedgerow, one sees the same reduced effectiveness with the windbreak row close to the house, but as the windbreak is planted far from the house (>150 mf), there is no apparent increasing AI tendency as distance increases. This means simply that a longer distance is required for the air downstream of the windbreak to remix with with unaffected air flowing adjacent to the windbreak stream of influence, since the hedgerow greatly reduced the directed kinetic energy of

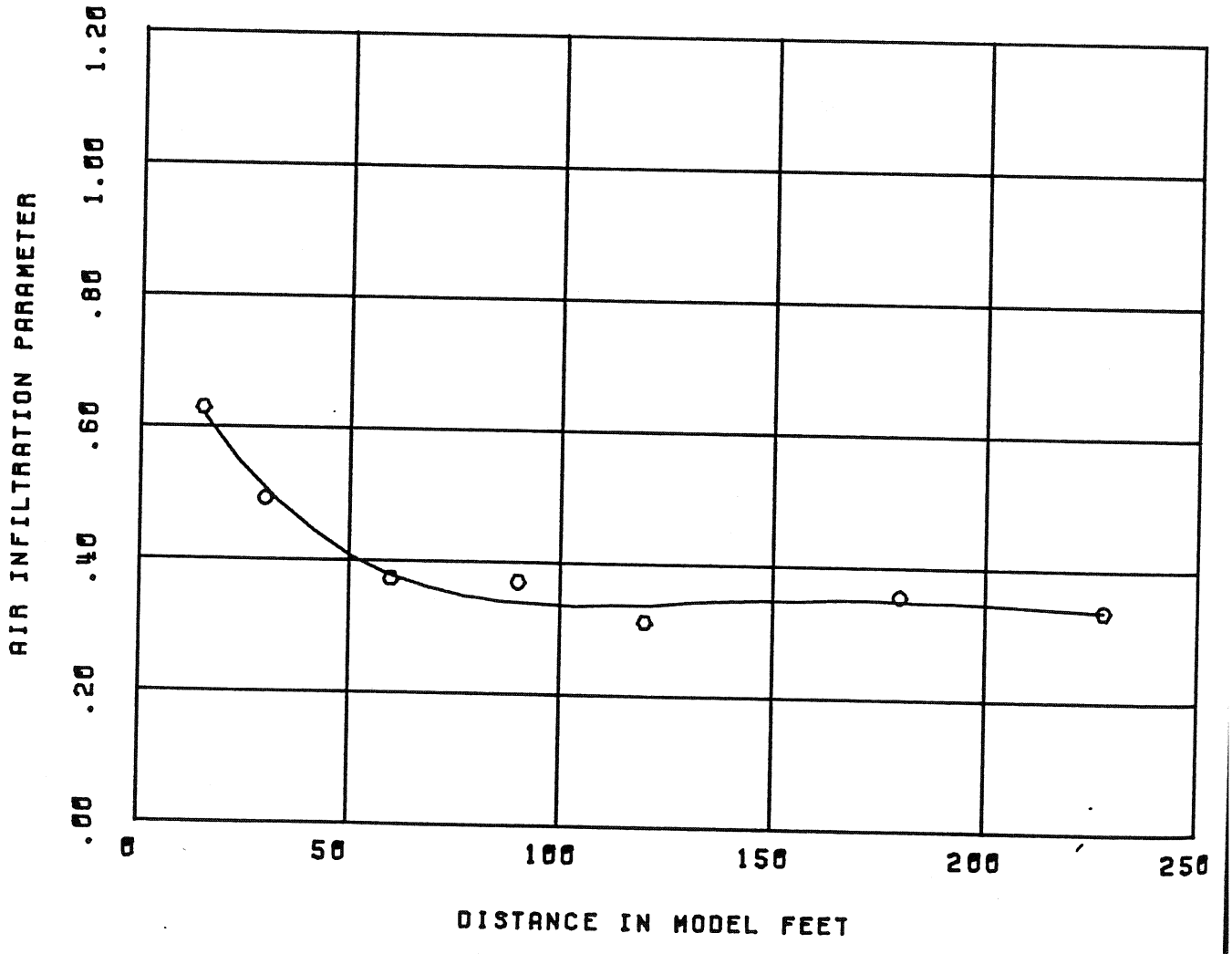

Figure 28: Plot of Hedgerow AI over Distance

the wind striking the house. In fact, there was such an energy reduction that the air flowing off the windward wall was moving so slowly as not to cause significant pressure drawdown at the windward wall edges, such as was the case with the open row and single tree(28). Maximum AI reduction achieved was 70% at 120 mf. A direct comparison of flow characteristics behind a hedgerow to no-tree flow characteristics can be seen in Figure 29.

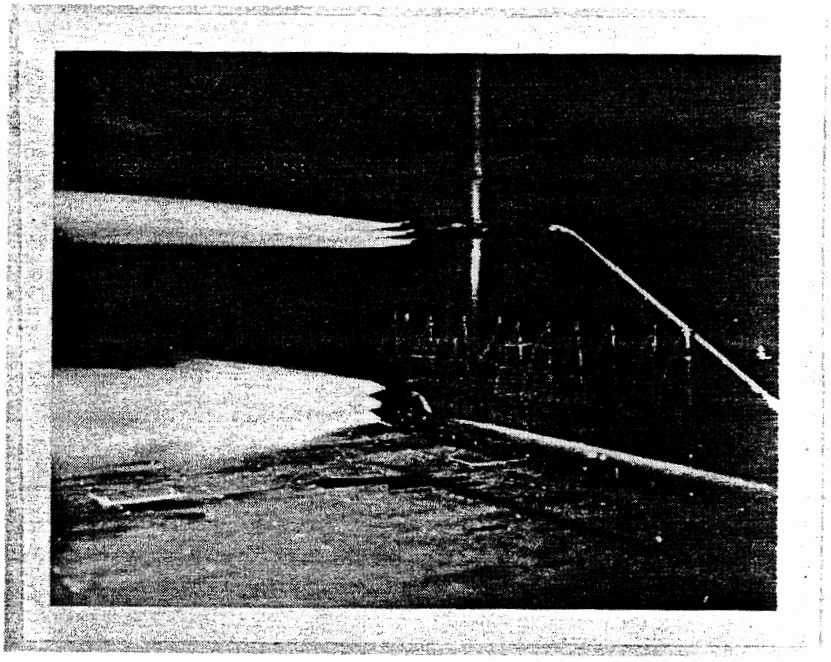

Figure 29: Comparison of Sheltered Flow with Unaltered Flow

The hedgerow configuration provides a small exception to the earlier statement about the non-flow-deflecting characteristics of naturally occuring trees. Figure 30a shows smoke flow through the tops of an open row, while Figure 30b shows smokeflow over the tops of a hedgerow. This deflection occured for all tree rows in which the tree crowns had grown together. Even with the extremely dense hedgerow configuration, however, deflection was found to be very small. It was concluded that for the scope of residential applications of windbreaks, trees afford protection mainly through turbulence generation.

---

28. CTPD, tests 37-41 compared with test 1 and tests 25-35

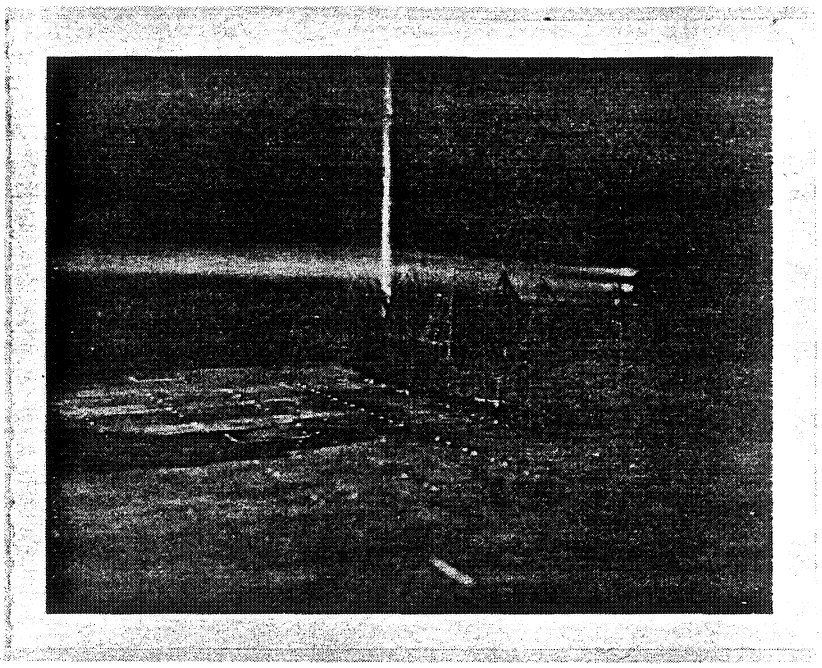

(a) - Non-Deflected Flow over the Top of an Open Row

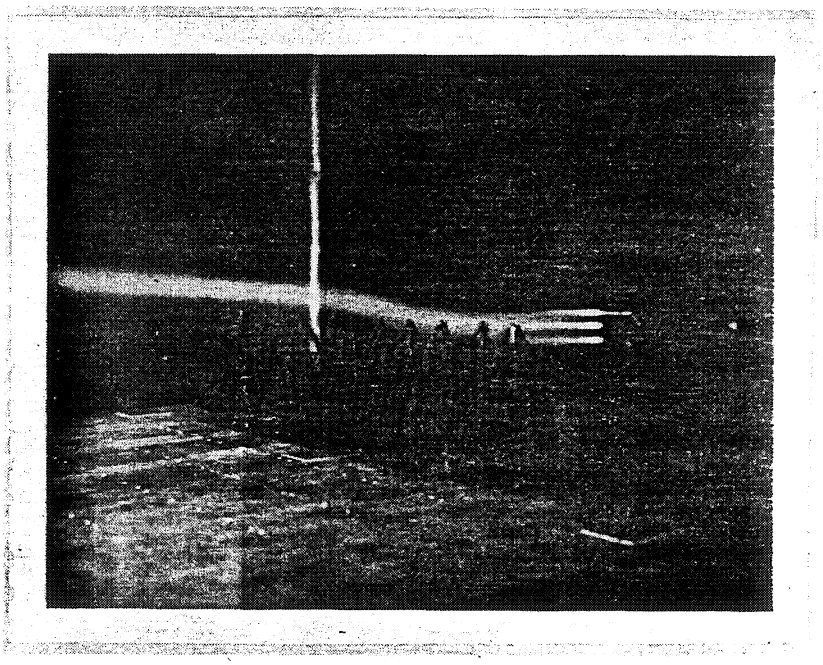

(b) - Deflected Flow over the Top of a Hedgerow

Figure 30: Flow Deflection Comparison over Various Types of Windbreak Rows

The open row AI versus distance tests were conducted on two separate occasions with different tree models constructed by identical methods.

Superimposed plots of these results are shown in Figure 31.. Clearly the results are substantially the same. The AI mean standard deviation among all the data shown is .09%, yielding a probable error of .06%, which is very low.

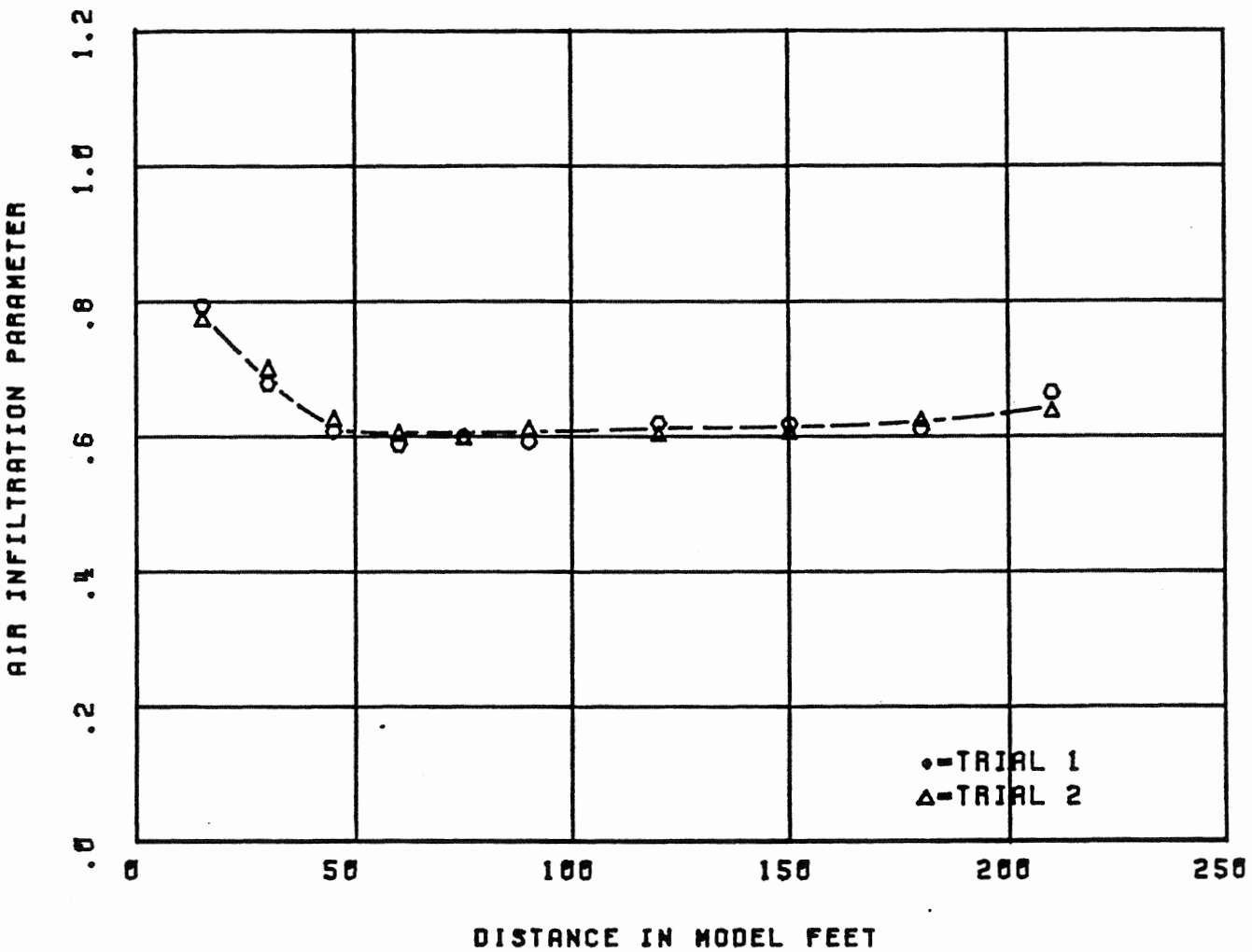

Figure 31: Repeatability Tests - Open Row AI over Distance

3.4 HOUSE ANGLED BEHIND A WINDBREAK ROW SERIES - (1,2,3,46,42,43,49,44,45)

The house was tested at three angles behind an open grown row and hedgerow windbreak. These results were compared with the House Alone Series results to determine if the ability of a windbreak to reduce air infiltration depended on the angle of the house behind it.

Figure 32 shows tests run with the house at three angles behind three different kinds of sheltering conditions: no trees, open row, and hedgerow. The AI figures for each run were normalized by the AI figure for the house facing normally for each of the shelter conditions (at 30 mf). The graph shows that between the house alone and the open row, the effect of rotating a house behind a windbreak is just a linear combination of the effects of placing the house behind the windbreak and rotating the house, both as explained before. For the hedgerow, wind velocity downstream of the trees has been so slowed that the contribution to AI of air being drawn out of the house by air flowby across a wall or roof surface is insignificant. AI appears only to be a function of form drag of the house, which decreases as angle increases. Figure 33 is a picture of the house angled at 45 degrees behind a hedgerow.

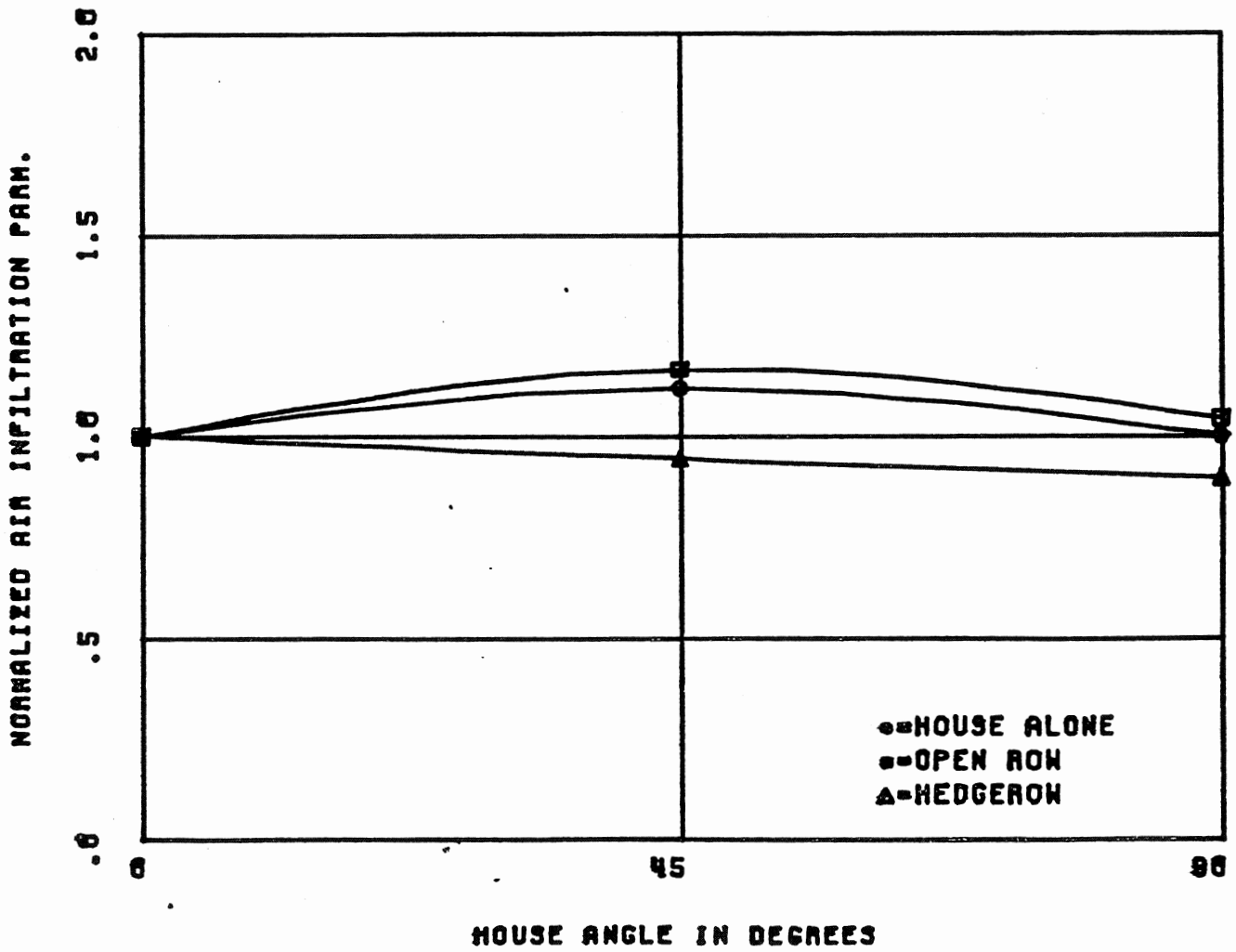

Figure 32: Normalized AI over House Angle for 3 Cases

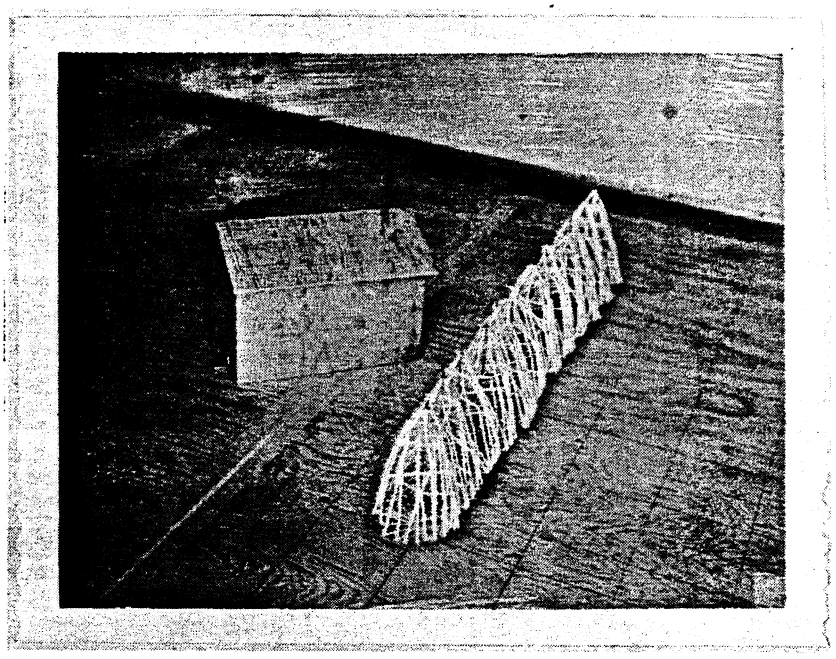

Figure 33: House at 45 Degrees Behind Hedgerow

3.5 SIDEWAYS EXTENT SERIES - (46,47,48,49,50,51,52)

An open row and a hedgerow of trees were tested at a constant distance of 30 mf upstream of the house with incremental numbers of trees removed from the ends of the house to determine the protective value of windbreak trees not directly upstream of the protected building.

This series simply reaffirms the statement made earlier with regard to the single tree, that trees only shelter what is directly downstream of them. Figure 34 shows a plot of AI over windbreak row length for a hedgerow. The plot shows that reducing the length of the windbreak down to slightly longer than the front wall of the house, whose length is 35 mf, has no effect. Again, longer windbreaks are useful in that they provide protection over a wider range of wind approach directions.

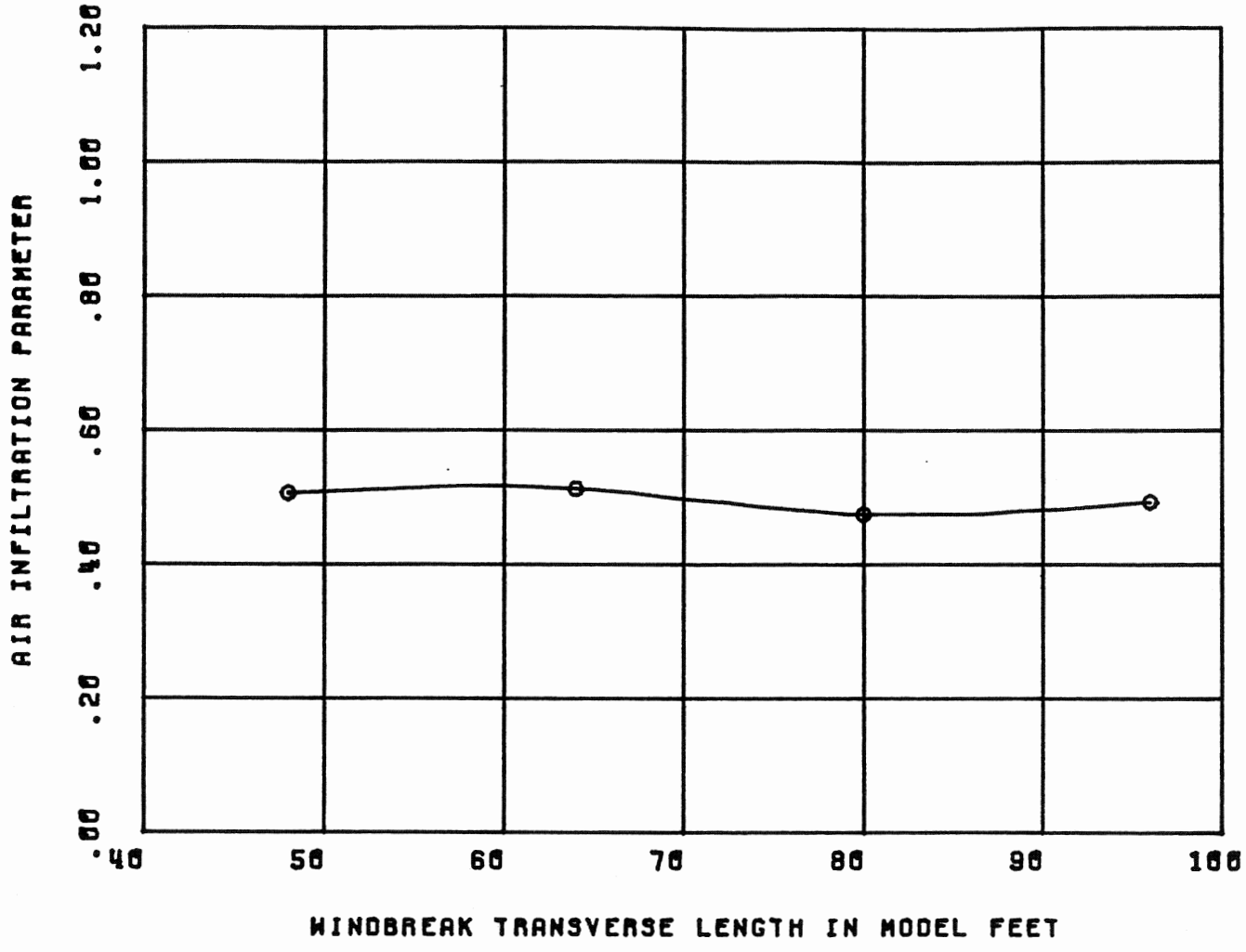

Figure 34: Plot of Hedgerow AI over Windbreak Length

3.6 DRAG SERIES - (46,53,54,55,56)

A row of trees of varying drag coefficients but with identical shape, spacing, and height was tested to determine marginal change of wind protection with tree drag, a concept that is often discussed in the literature(29).

The series yields an intuitively predictable result; AI decreases as the drag coefficient of the trees used in the windbreak increases. Figure 35 shows this graphically. The configuration used for testing was the open row. A picture of the drag test setup for .92 drag coefficient trees is shown in Figure 36. With trees of very high drag coefficient, small amounts of flow deflection were observed.

---

29. Meroney, R. N., p. 780

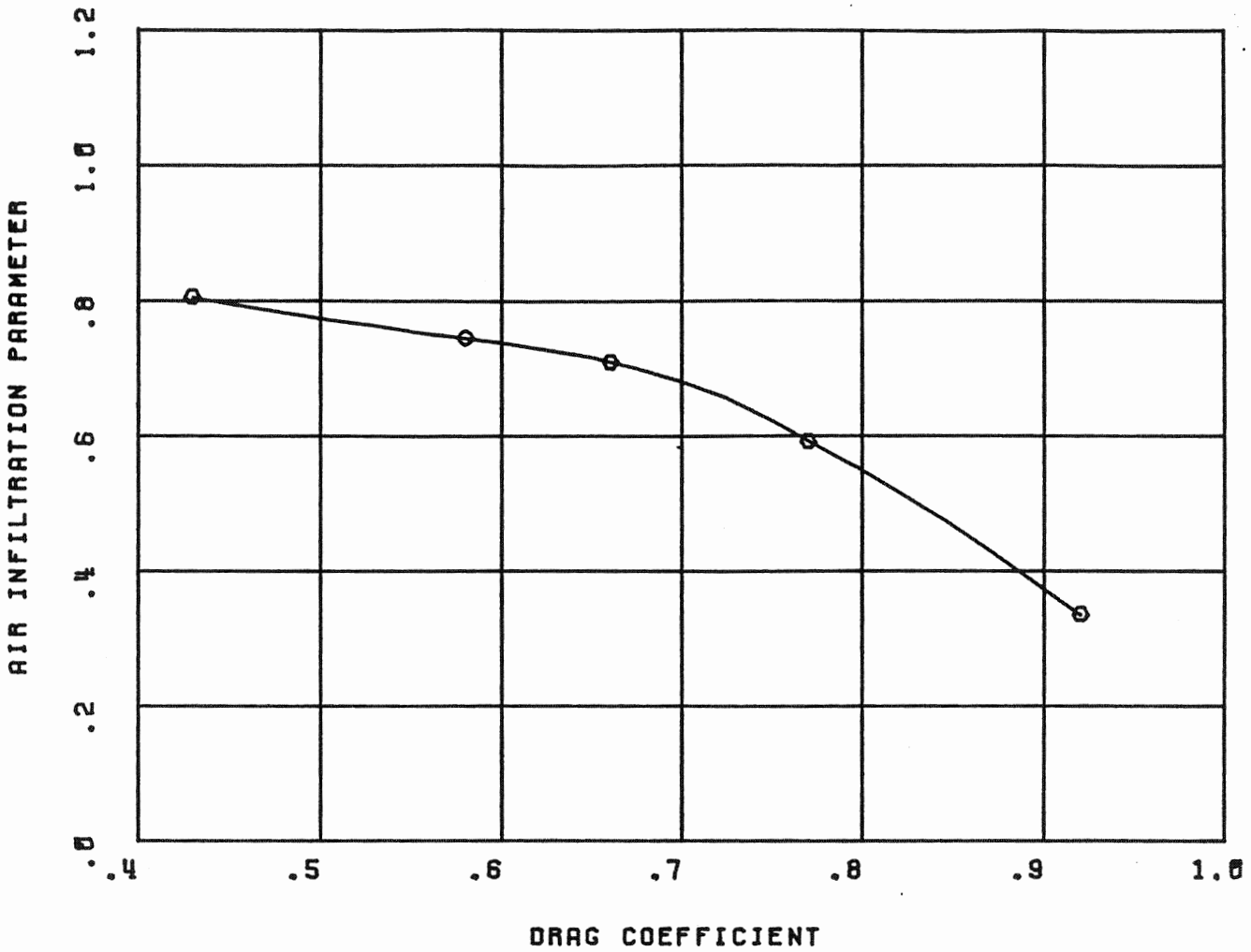

Figure 35: Plot of Open Row AI over Tree Drag Coefficient

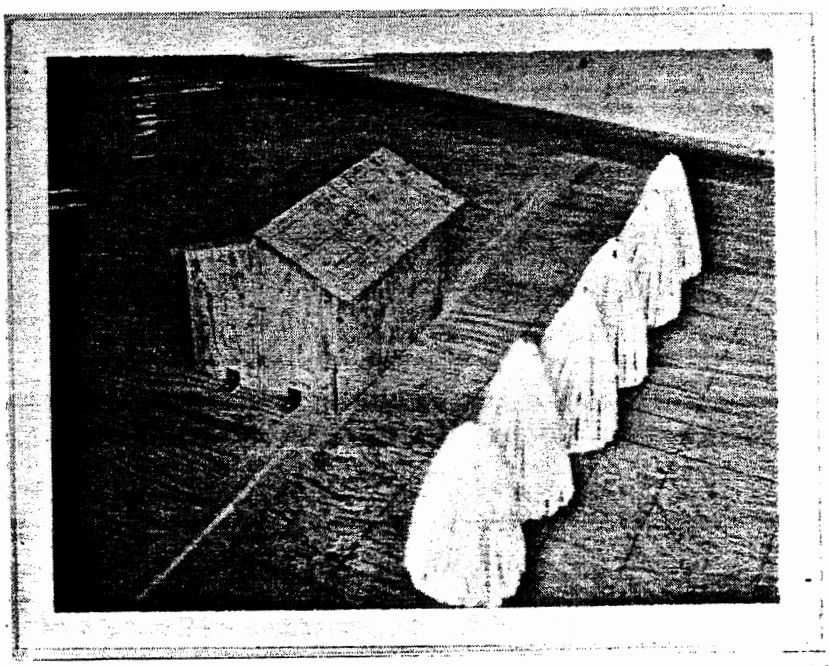

Figure 36: House Behind Open Row of .92 Drag Coefficient Trees

3.7 LATERAL SPACING (SPECIAL) SERIES - (46,49,57,58,59,60,61)

A row of trees was tested at constant distance upstream varying the lateral planting densities from a very dense hedgerow to a sparsely planted open row, to determine the marginal gain attributable tc planting denser windbreaks.

This series also confirms an intuitively reasonable concept; AI decreases as windbreak row planting density (in trees per model foct cf row length, where the trees are all of standard drag coefficient) increases. This is graphed in Figure 37. The inflection point in the otherwise linear curve occurs when adjacent trees are spaced so that tree crown tips are just touching. This is also intuitively reasonable. Moving open grown trees closer together linearly decreases the treeless cross sectional area between them at a constant rate. Cnce the tree crowns have begun to merge, this rate begins tc slow as the cross sectional area of each tree beccmes effectively smaller as the trees are moved

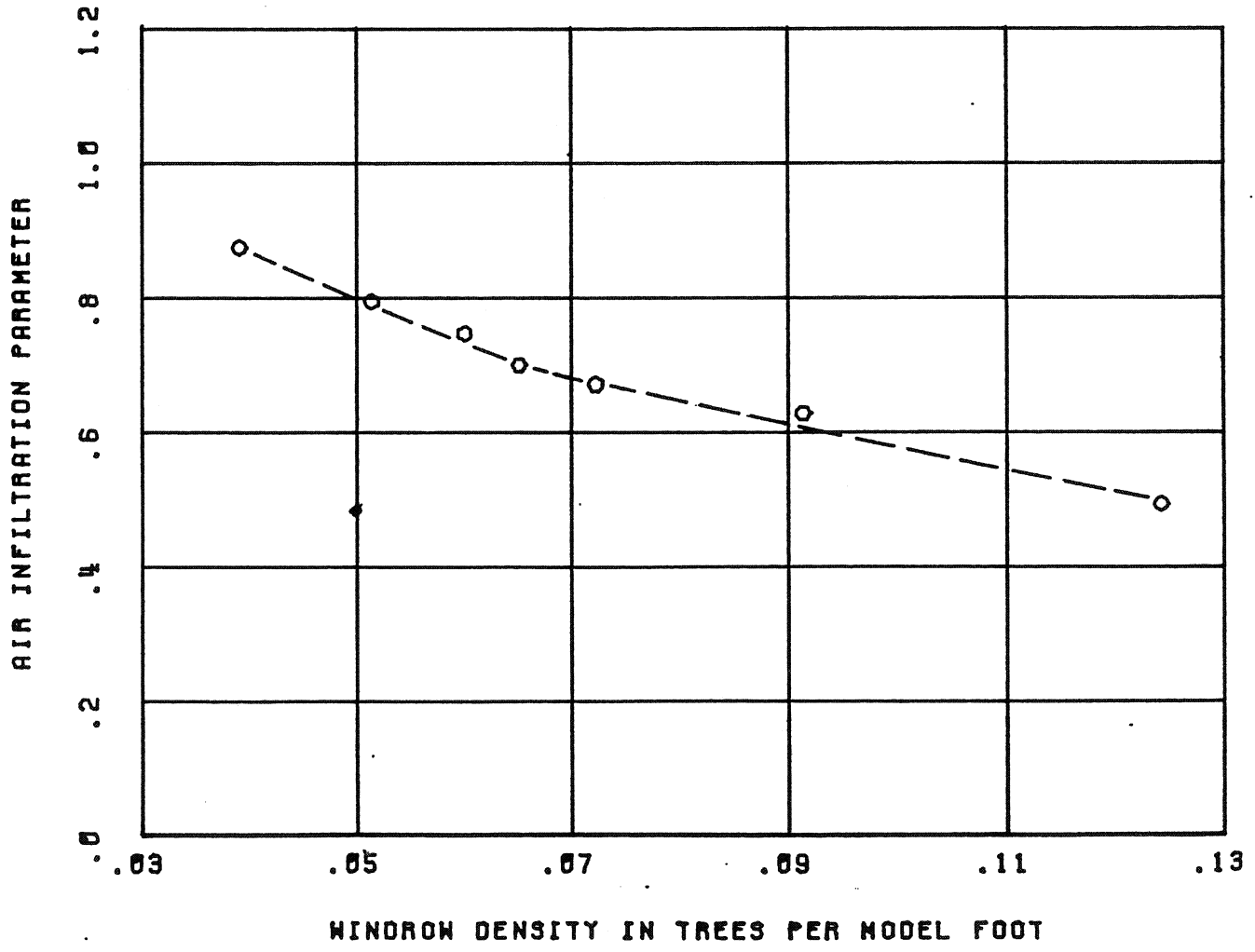

Figure 37: Plct of AI over Windbreak Row Density

closer together. This lost cross-sectional area is not made up by increased local drag coefficient in the merged area; the foliage there withers through intolerance. Thus, planting trees with merged crowns is relatively inefficient when one considers the additional number of trees required to cover a given windbreak row lineal footage.

3.8 HEIGHT VARIATION AND ROW STAGGERING SERIES - (46,62 THROUGH 70)

Trees of the same type and varying heights were tested to determine the marginal effect of increased tree heights. These tests were conducted with the trees planted in both an in-line and staggered windbreak row, to determine the differences in protection afforded by the two plans, and if such differences varied through the growth cycle of a tree.

The results of this series are also reasonable. As trees grow taller and therefore larger all around, the AI of structures protected by them decreases. This is shown in Figure 38.

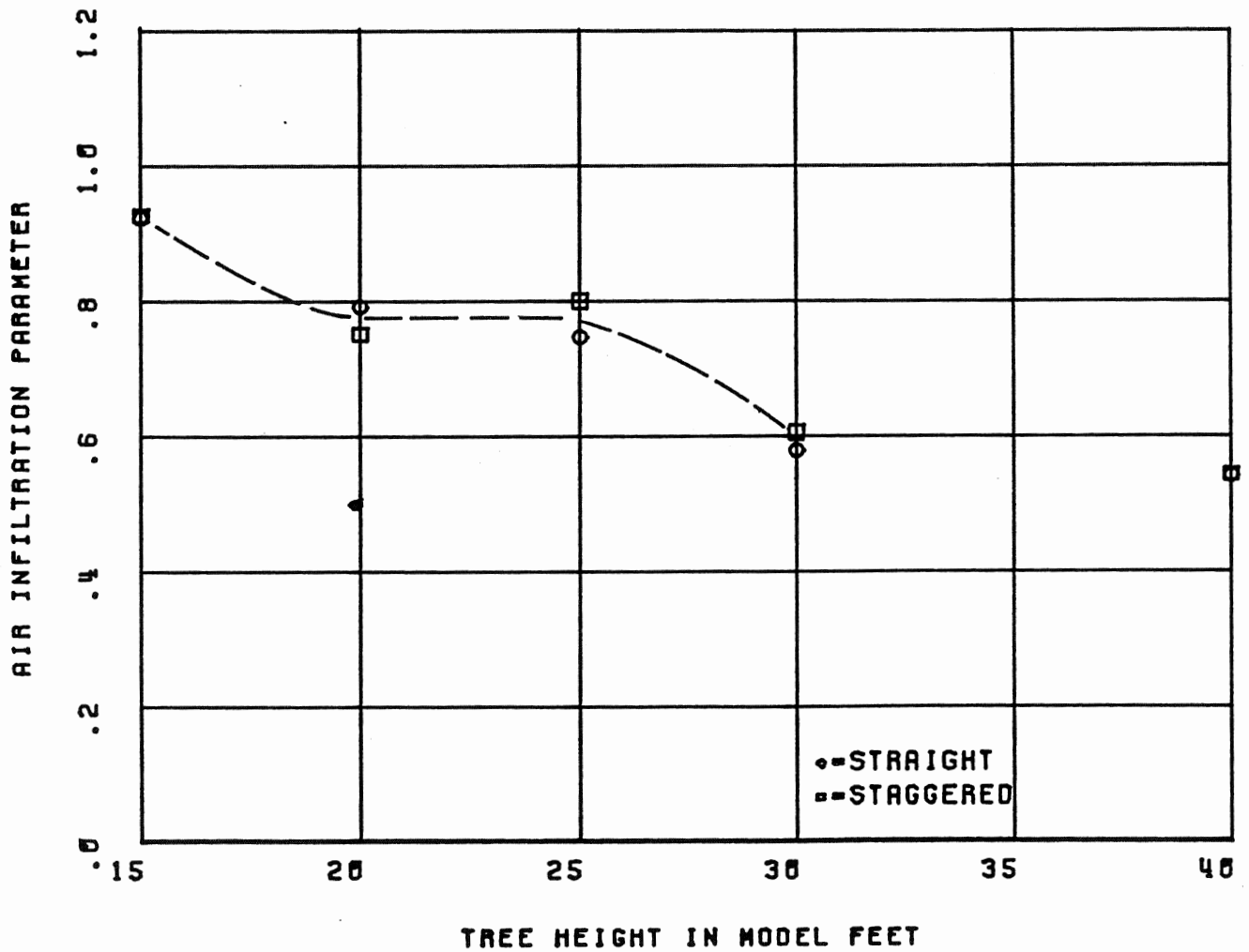

Figure 38: Plot of AI over Open Row Tree Height

As is shown in Figure 39, when the trees were staggered for the staggered versus non-staggered comparison, lateral row density was held constant. That is, every other tree in the row was simply moved 15 mf upstream. In keeping with the idea that trees do not deflect but merely slow air passing through them, no appreciable difference exists between the staggered and non-staggered cases. This is of momentous import as it allows the windbreak planter to space trees in the direction of the oncoming wind at will, or perhaps as needed to meet light-and-air ordinances, which are now in effect in many communities (30).

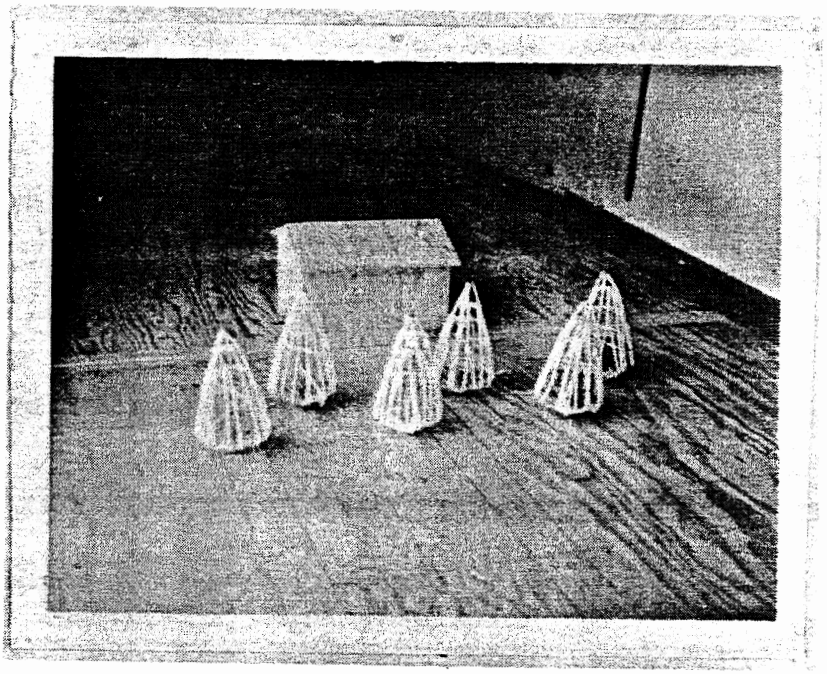

Figure 39: Picture of Staggered Row Test Setup

---

30. One example are the ordinances of Princeton Township, Mercer County, New Jersey.

3.9 INCREMENTAL ROW SERIES - (47,71,72,73,74)

The effect of double and triple row windbreaks with and without side staggering of the second row were tested for comparison of performance with single row windbreaks.

These tests, whose plan views are shown in Figure 40, show two trends. First, starting from the center panel and proceeding down the left-hand side of the figure, it is apparent that extra rows of trees do reduce AI. Proceeding from the center down the right, it is shown that staggering alternate rows improve protection row for row. These results are excellent logical extensions of the idea that the protection to a building afforded by trees is related first and foremost to the amount of tree foliage between the sheltered building and the oncoming wind.

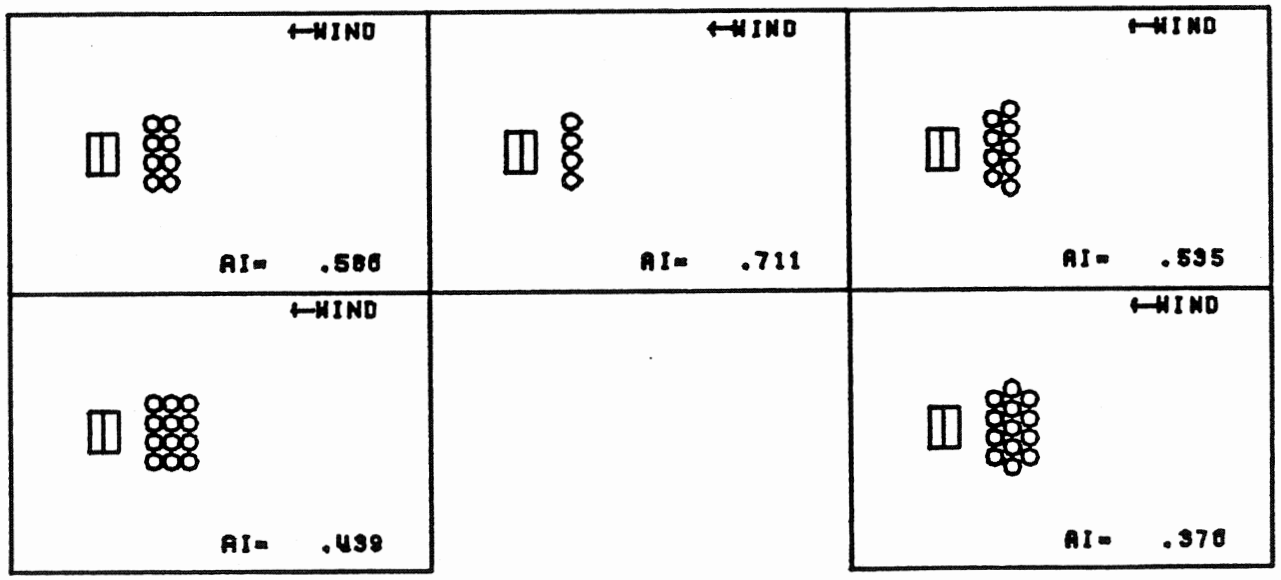

Figure 40: Incremental Row Tests

3.10 UNDERPRUNING SERIES - (75,76,77,78,79,80)

A row of trees without lower branches was tested, varying trunk lengths below the crown. These trunk lengths varied from 20 feet longer than naturally occuring to no trunk below the crown at all. The purpose of this series is to determine the usefulness of raised canopy trees as windbreaks.

Figure 41 shows how windbreak trees without lower branches decrease their protection as the tree crown separates from the ground (longer trunk). Indeed, for tree crowns grown together whose bottoms are very nearly the same height as the roof of the house, a deleterious effect may be seen.

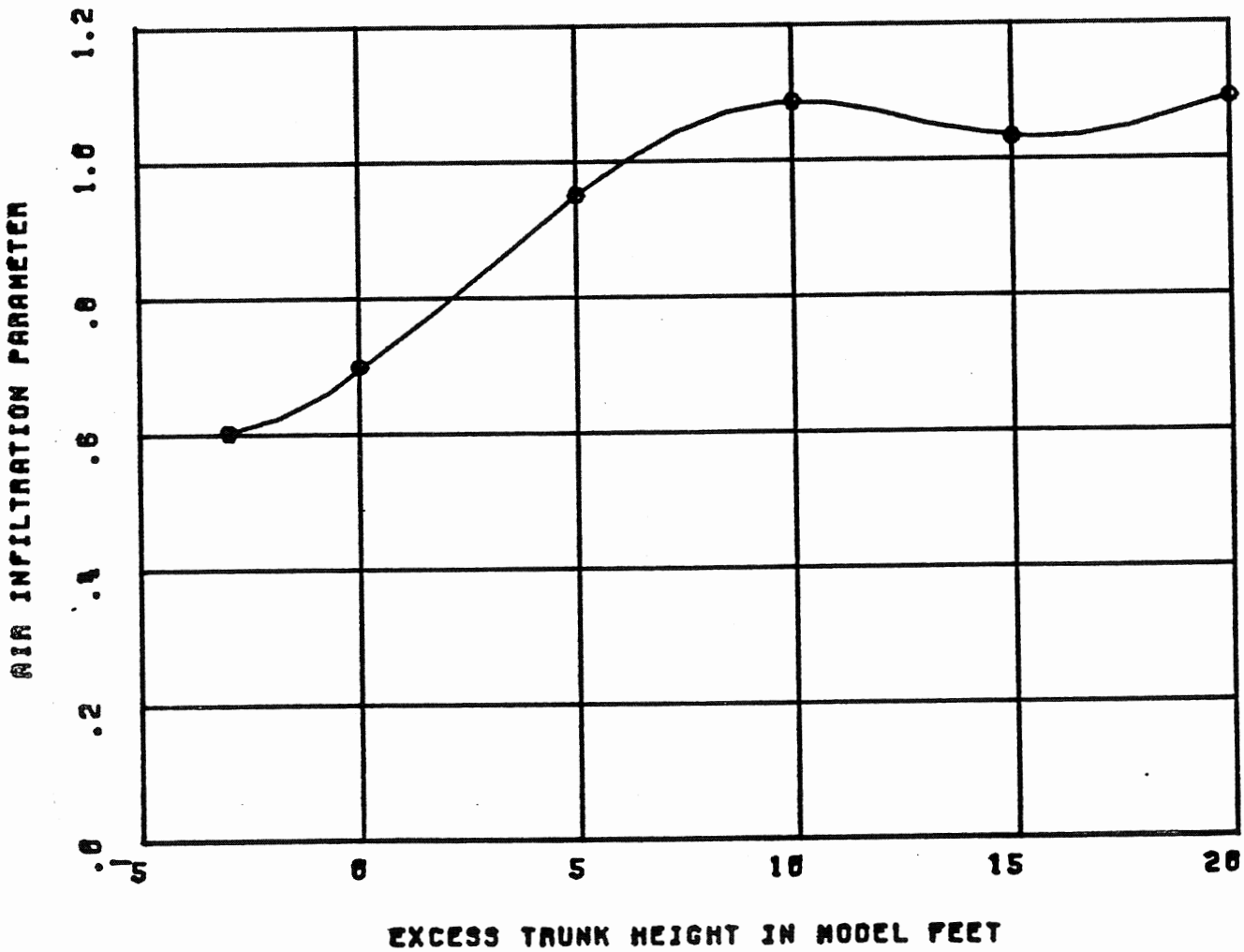

Figure 41: Plot of AI over Excess Trunk Height

The reason for this is demonstrated in Figure 42. In Figure 42a, one sees a smoke trace of air flowing over the front roof panel of a house with no trees. Figure 42b shows what happens when, without moving the smoke rake, trees are put in place whose merged crowns selectively abate wind striking the windward roof, and deflect air slightly onto the windward wall. The net effect of this is that the net velocity of the air as it flows of the windward wall is more upward, increasing separation off the windward roof, which increases the pressure drop across that surface. This phenomenon is verified by the pressure coefficient distributions in the CTPD(31). This condition is further aggravated by moving the crowns five feet downward to more squarely block off air to the windward roof, as shown in Figure 42c..

Figure 43, on the other hand, shows the most favorable test of the Underpruning Series, the test with the tree crowns located as close to the ground as possible. In this case, a stagnation zone has built up from the house to the trees. Thus, flow that would normally strike the windward wall flows neatly and smoothly over the roof. This test shows by far the lowest front wall pressure of any in the series. Such an arrangement, which gives a reduction similar in magnitude to the open row while being of less stature and closer to the house, indicates how low-profile windbreaks such as hedges of bushes might be used.

---

31. CTPD, tests 75-78

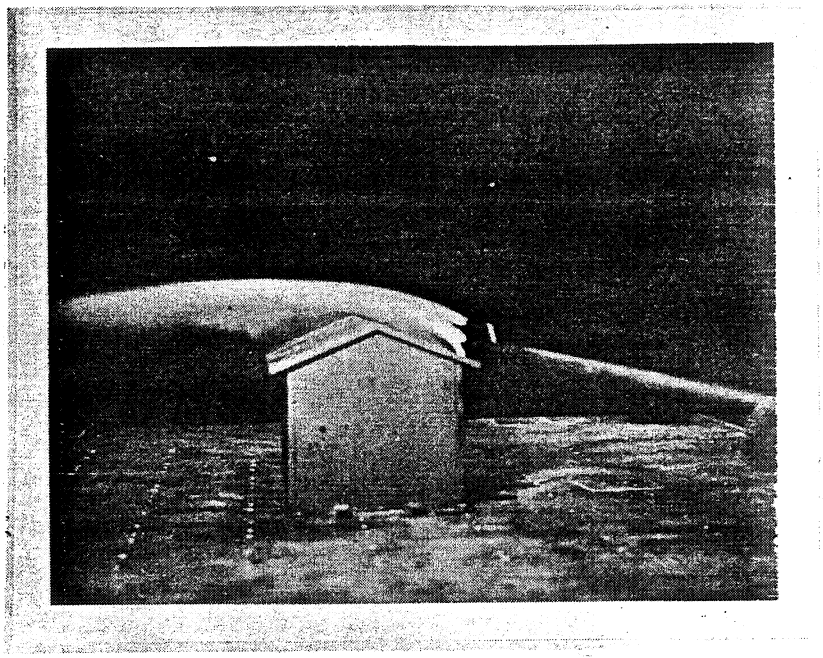

(a) - Flow Over Windward Roof With No Trees

(b) - Separated Flow Over Windward Roof with 20 Foot Excess Trunk

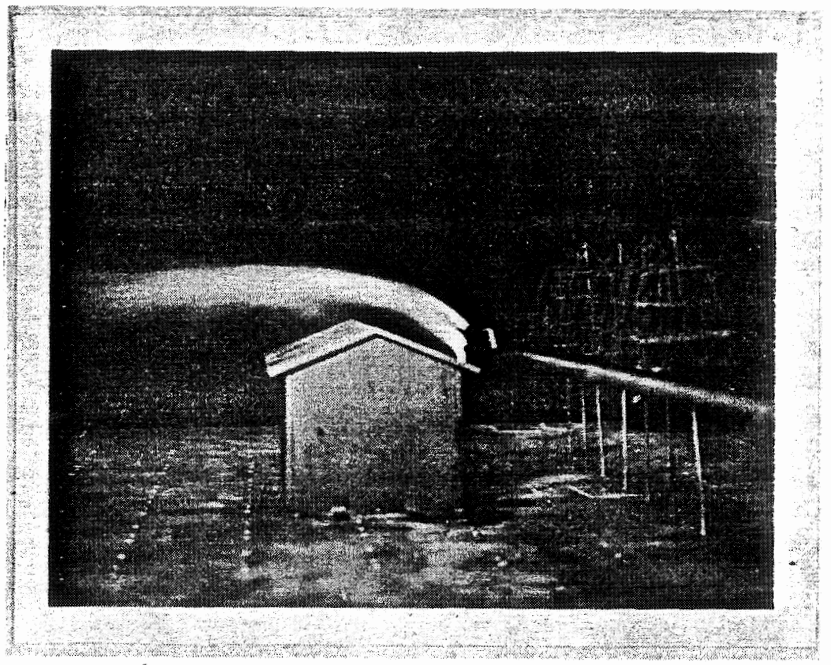

(c) - More Separated Flow with 15 Foot Excess Trunks

Figure 42: Flow Separation With Increased Bare Trunk Height

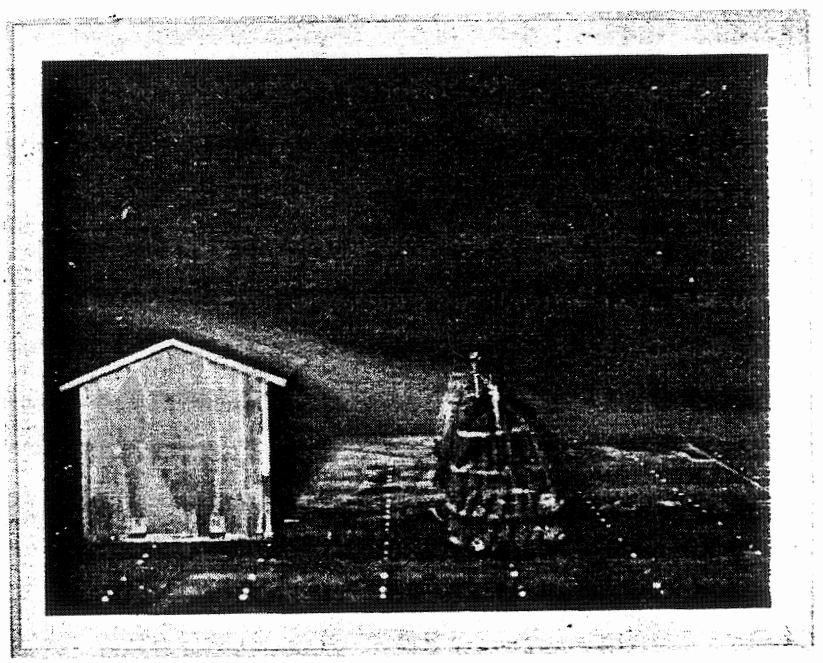

Figure 43: Launching of Windflow over House Using Low-Profile, Close Proximity Trees

3.11 FORE/AFT SERIES - (46,81,82,83)

The effects of a second row of open grown trees at various distances downstream of the house in conjunction with a row of trees located upstream of the house were examined to see if low pressure conditions on the leeward wall of the house might be alleviated by placing a second stagnation barrier to trap air.

These tests (shown in Figure 44) show that there is no improvement to be gained by planting additional rows downsteam of an already protected house. The differences in AI in Figure are probably due to experimental variation. This confirms the previous deduction that air infiltration is affected primarily by conditions upstream of the windward surfaces of a house, through which the majority of wind-induced air in-and exfiltration takes place.

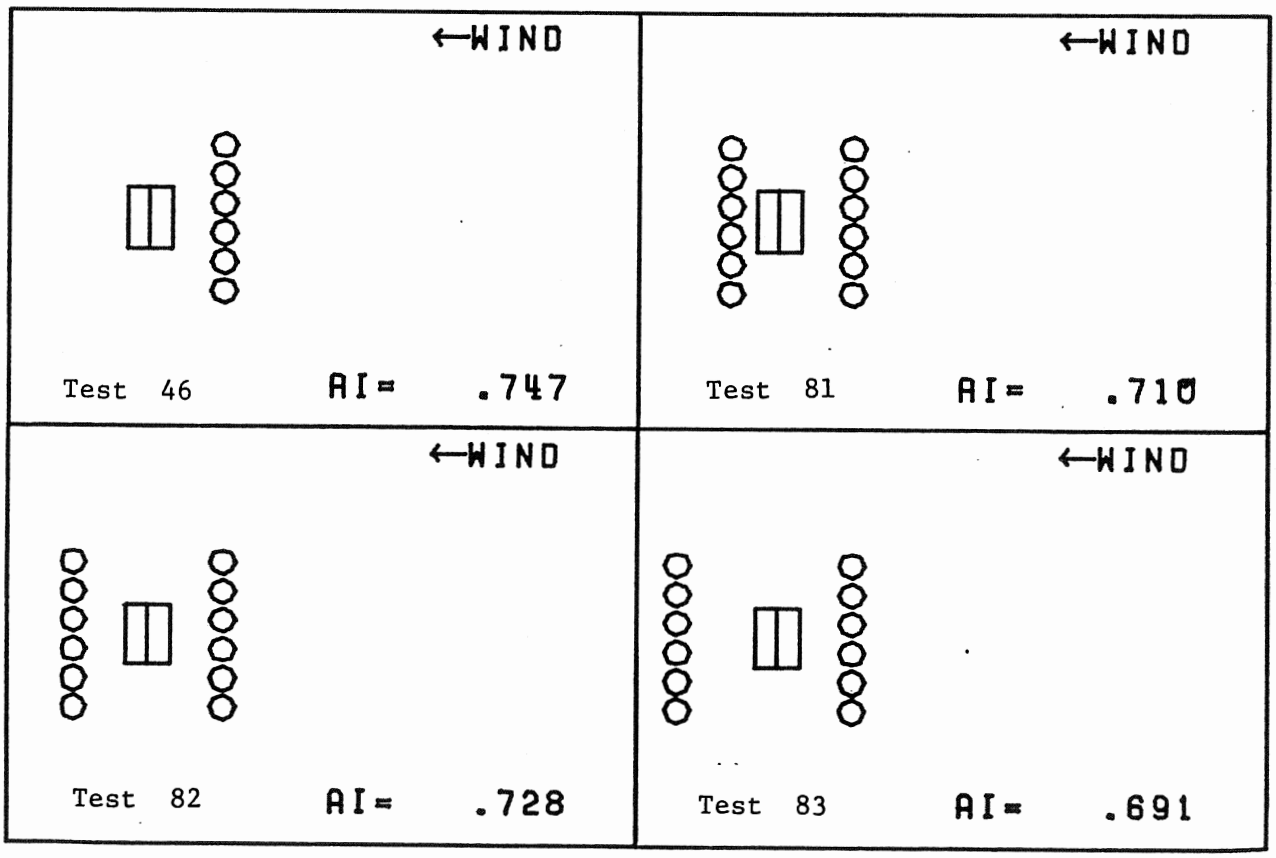

Figure 44: Plan Views of Fore/Aft Tests

3.12 SIDE ROW SERIES = (3,84,85,86,87)

The effects of having wind running parallel to a windbreak row were studied.

The plan views of these tests are shown in Figure 45. This series demonstrates that no deleterious or beneficial effects are encountered when wind is channeled between a house and a windbreak row. Again, the small variations seen in the figure are not significant.

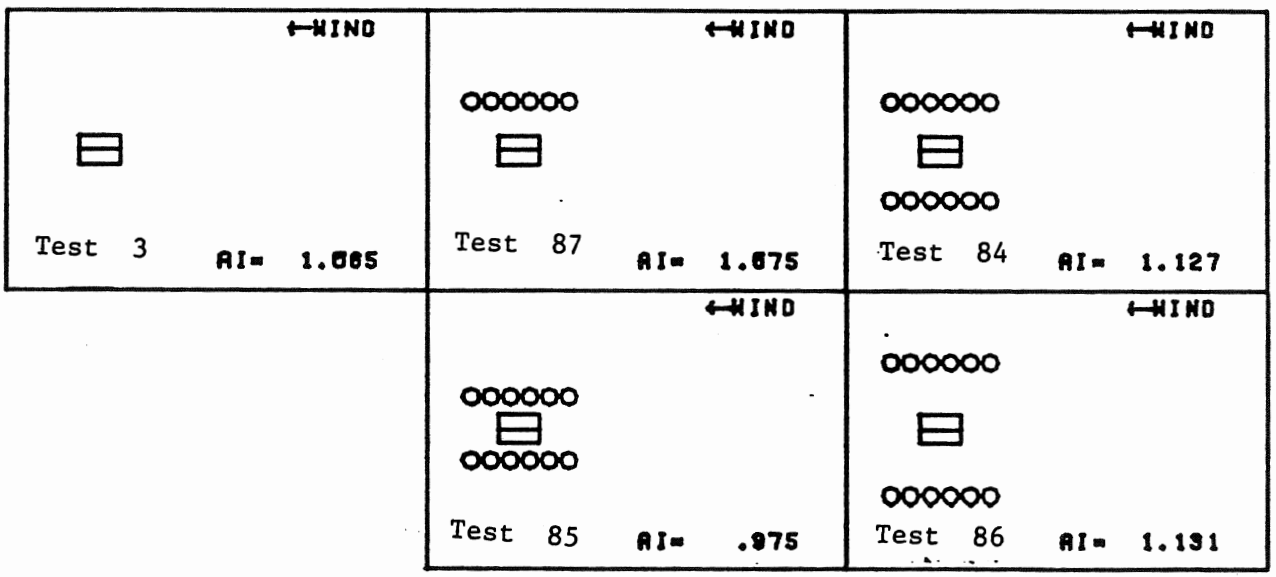

Figure 45: Plan Views of Side Row Tests

3.13 CONTOUR BOX SERIES - (88,89,90)

The effects of surrounding the house with 4 rows of trees, one parallel to each side of the house, with the house situated at three angles with respect to the approaching wind were tested.

These tests, whose plan views are shown in Figure 46 compared with their unprotected counterparts, were conceived to see if a windbreak planting which merely followed the form of the house it protected around the entire house perimeter would protect equally well over a wide range of directions of wind approach.

Such is the case, with reductions of approximately equal magnitude all around. The reductions achieved, however, are not quite as high as those achieved through the planting of a well placed open row in the windward direction. So, while the Contour Box is a good, general purpose, first-approximation shelterbelt, according to the findings discussed previously, it contains excess trees which render it less efficient in situations characterized by prevailing winds. Its picture is shown in Figure 47.

To be more effective, a shelterbelt should be tailored to the sheltering situation for which it is intended. How this is accomplished will be explained more fully in the Application of Results section, which follows.

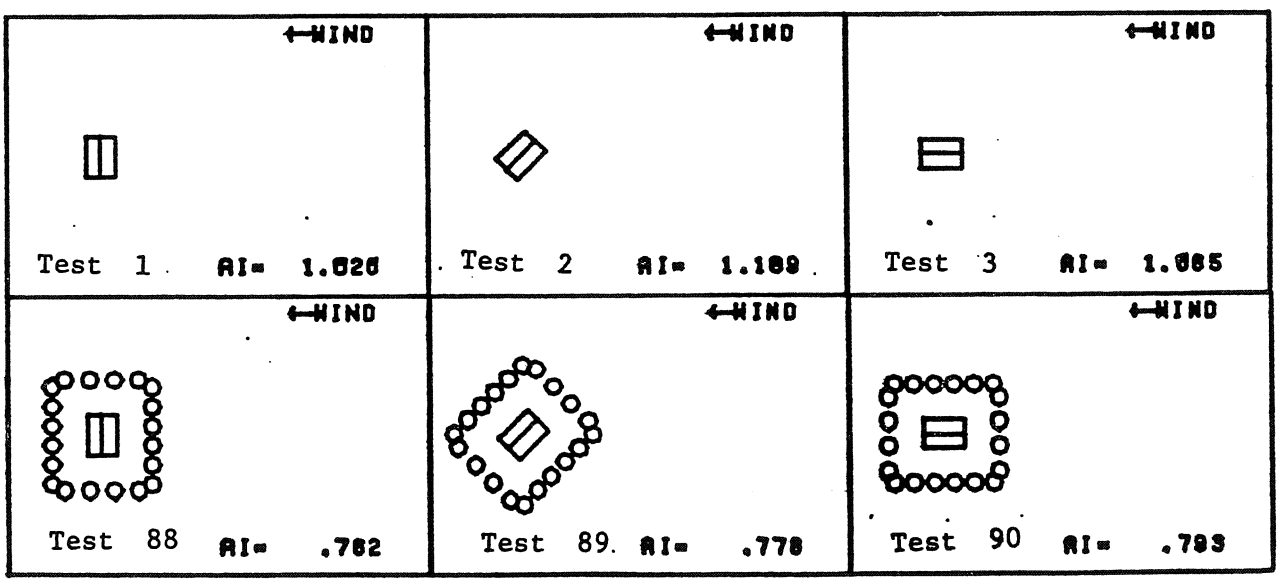

Figure 46: Plan Views of Contour Box Series Tests as Compared To Unprotected Trees at Similar Angles

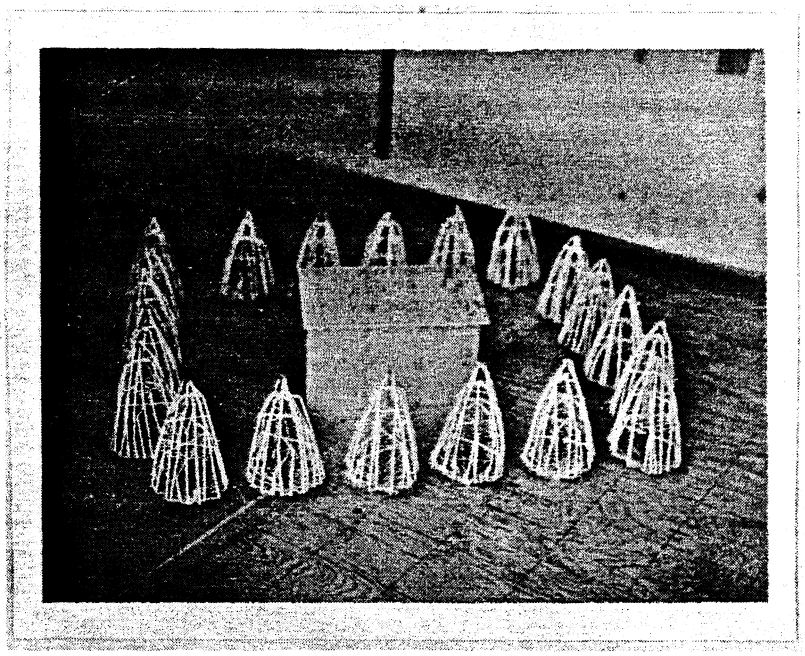

Figure 47: Picture of Contour Box Test

3.14 LEADING WEDGE SERIES - (91,92,93,94,95,96,97,98,99,100)

The effects of a wedge of trees (3 trees) planted upstream were tested and compared to the row windbreaks discussed previously.

The leading wedge tests show the same type of upstream range of maximum influence (Figure 48) as did the single tree (Figure 23), open row (Figure 26), and hedgerow (Figure 28). Maximum influence extends from 60 to 120 mf. The maximum reduction achieved was 53% at 90 mf. This is significantly better than an open row, which is reasonable since the leading wedge is composed of three trees which, if collapsed into an in-line row, would form a row of overlapping trees much like a hedgerow. A leading wedge arrangement is shown in Figure 49. The leading wedge performed better than the open row for the same reasons that the multi-row or higher planting density tests did in that it puts a denser amount of tree foliage between the house and the oncoming wind. The leading wedge, however, as with the single tree, is good for winds from one direction only. Its use is therefore limited to special applications, usually those requiring low-cost protection from a prevailing wind.

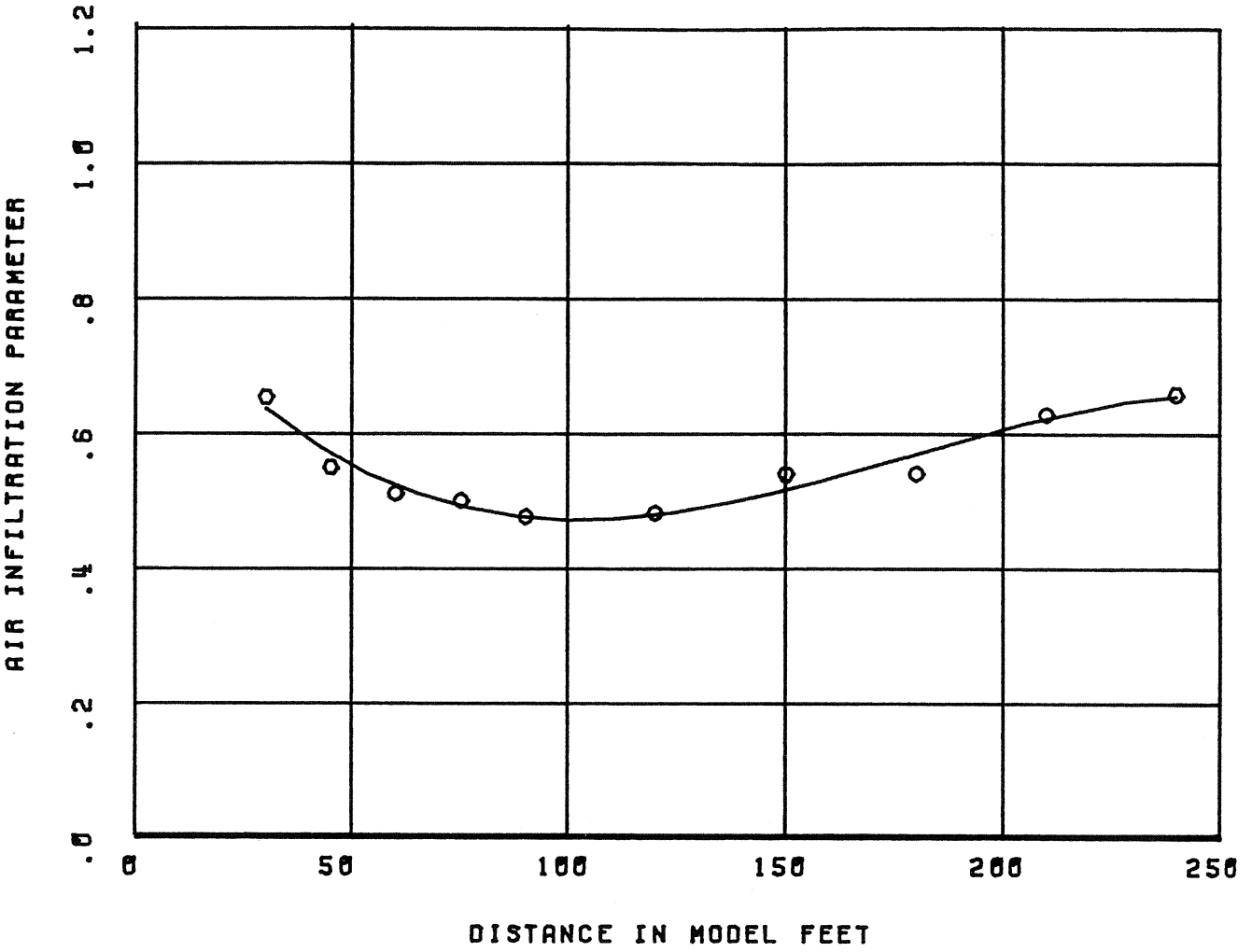

Figure 48: Plot of Leading Wedge AI over Distance

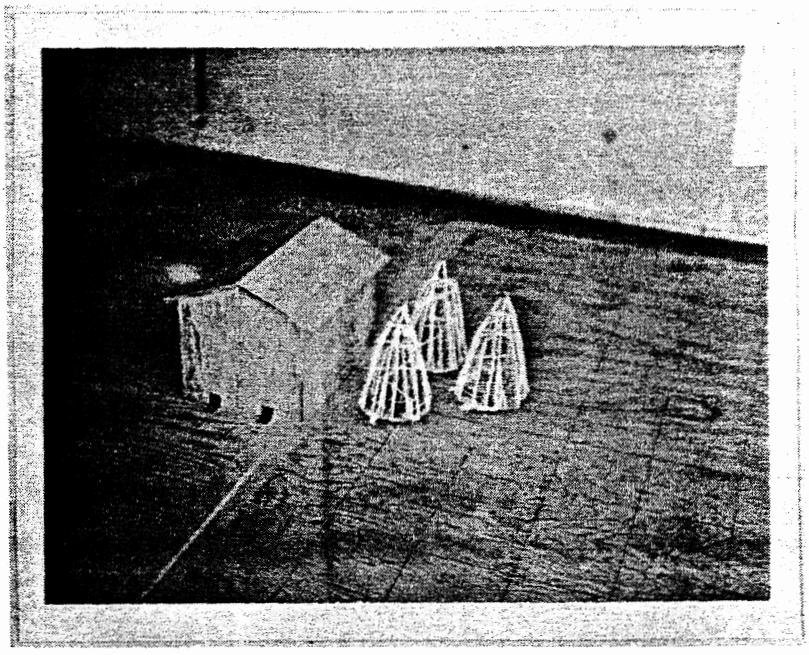

Figure 49: Leading Wedge Configuration

3.15 DRIVEWAY SERIES - (101,102,103,104,105,106,107,108)

The effects of a gap in a hedgerow windbreak where the gap lies directly upstream of the house, and of various methods for reducing the problems associated with this gap, were tested. Plan views are shown in Figure 50.

This series was conceived to try to find a solution to the problem of wind pouring through a windbreak where a driveway or stream must pass. In the top, left-hand panel, a driveway opening has nearly doubled the AI from the no opening case of .374 to .740.

In the remaining panels, it is seen that resolution of the problem may be accomplished in more ways than one. In keeping with the previous conclusion, it is also seen that the degree to which AI is reduced is proportional to the number of trees planted in the wind corridor in which flows the wind that blows against the house. Even though, in the bottom right-hand panel, the patch-up trees are planted very far up- and downstream of the windbreak gap, this test yielded the maximum AI reduction of <u>every</u> test run in the entire study, with an AI reduction of 72%, and this was achieved even with the main hedgerow not planted in the optimum upstream position as determined in the hedgerow tests of the Distance and Repeatability Series.

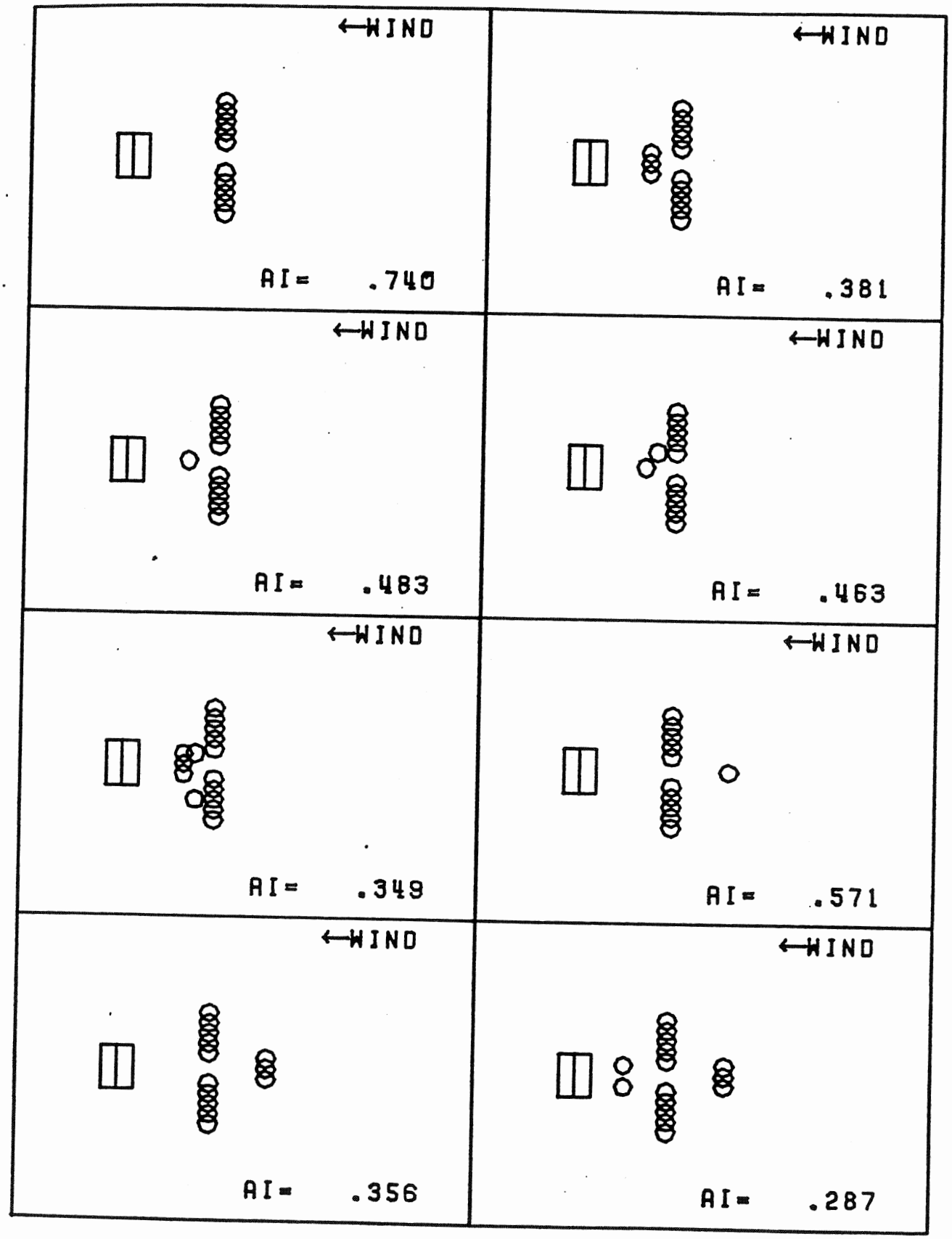

Figure 50: Plan View of Driveway Tests

4. APPLICATION OF RESULTS

The ways in which various input factors influence AI reduction have been discussed. The question now to be answered is how to put the information given into practice. A description of one method follows.

Information on average wind speed and direction distributions is available for most locations in the United States through the National Weather Service(32). The data are often presented in the form of a "wind rosette" such as the one for the winter season in the Trenton, N. J. area shown in Figure 51(33). The rosette divides the wind approach direction continuum into 8 ranges, and gives the percentage of time the wind blew from each direction (bar lengths), and the mean velocity at which it blew (numbers). Reading from the figure, wind blows through the Trenton area from the north about 17.5% of the winter at a mean velocity of 9.6 mph.

The results derived from this study present AI parameters for wind blowing from particular directions due to trees being planted about the protected house a certain configurations. To accurately relate AI parameters to heating energy savings, it is necessary to take into account wind direction and windspeed.

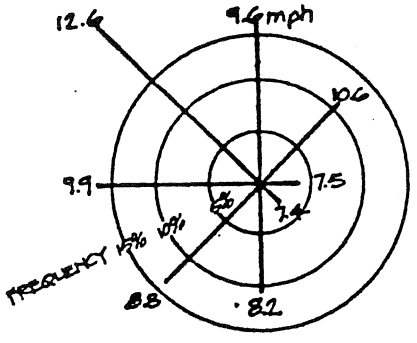

WINTER (Dec-Jan-Feb)

Figure 51: Wind Frequency Rosette for the Trenton, N. J. Area

---

32. National Climatic Center, Asheville, N. C.

33. Chaney, T., Golden, F., Maxwell, I., and Rogers, J., "A Natural Resource Inventory of the Stoney Brook Watershed, Mercer and Hunterdon Counties, New Jersey", a Master of Regional Planning Report for the Graduate School of Fine Arts, University of Pennsylvania, 1974

In full scale studies using townhouses at Twin Rivers, N. J., it has been observed that the average air infiltration participation in heat losses is approximately one third at an average windspeed of 10 mph. Wind causes about three quarters of this infiltration under open site conditions. Thus the wind causes about one quarter of total heat losses at average windspeed. It stands to reason that when the windspeed is zero, then the wind contributes nothing to heat loss. It was also shown that at 20 mph, air infiltration accounted for more than half of the heat loss rate. These three windspeed/heat loss relations specify a power law heat loss function over windspeed. This function solves to be:

$$HL(w) = HL_0 \, F(w)$$

$$= HL_0 \, (2.216 - (1.478 - .0730 \, P \, w)^{.5})$$

where HL(0) is the heat loss rate coefficient determined from the home heating bill, w is the windspeed in mph, and P is the house protection coefficient. When the house is totally exposed to the wind, P=1, and when the house is totally protected from the wind, P=0. Thus, in the context of this study:

P = 1 - fractional AI reduction.

A plot of HL(w) for various values of P is given in Figure 52.

Over the heating season, heat energy cost equals heat energy lost integrated over the time of the heating season. This integral may be expressed as a summation over the 8 approach directions in the wind rosette of the heat loss rate which would occur were the wind to blow from that direction at the average windspeed of that direction, multiplied by the percentage of time wind came from that direction. If one assumes a proportional relationship between fuel costs and heat energy used, the expression for heat cost over a heating season is:

$$\text{Heat Cost} = HL_0 \sum_{d=1}^{M} F(w_{av}(d), P(d)) \; Freq_{av}(d)$$

where w(av)(d) and Freq(av)(d) are the average windspeed and percentage time wind was blowing for the direction d and M is the total number of wind approach directions. A homeowner may calculate the HL(0) for his particular home by evaluating the summation for his meteorological area using P values that reflect the layout of trees surounding his home. The summation value is divided into the heating cost paid for the previous heating season to yield HL(0).

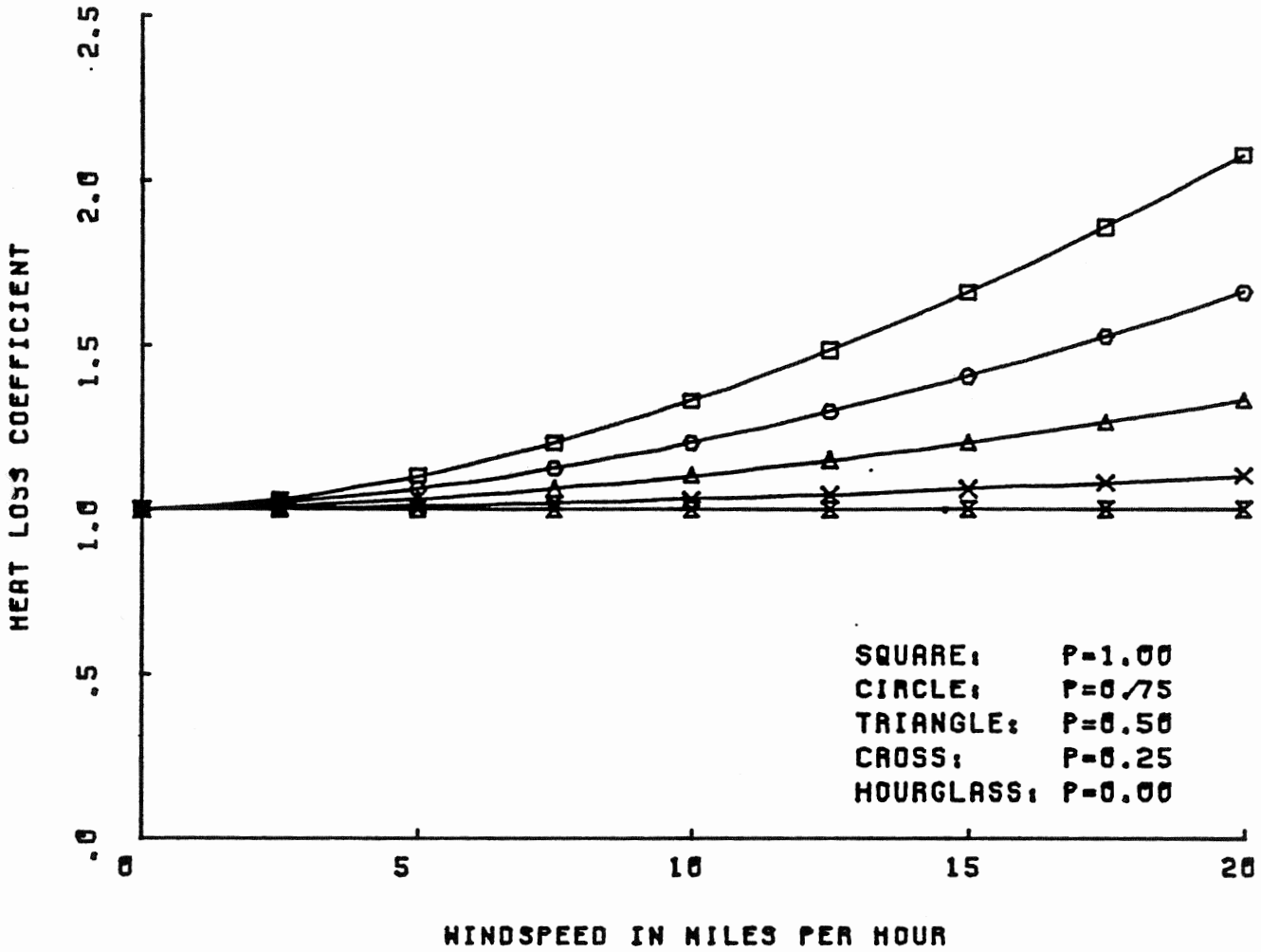

Figure 52: Heat Loss as a Function of P and Windspeed

The homeowner then takes the summation and evaluates it using the HL(0) calculated previously and P values for each direction that reflect the kind of windbreak that is desired for each direction. This will produce a predicted heating cost, which the user may subtract from his previous heating cost to determine savings. The process is repeated a number of years into the future taking into account that heating costs will inflate and that the trees planted will grow. The accumulated savings are applied to the price of planting the trees involved to determine the payback period for the windbreak and the eventual net monetary savings.

To determine the P values for use in the summation calculation, one selects the kind of tree windbreak desired to protect a given wind approach direction, and one calculates the fractional AI reduction from the unprotected case offered by that windbreak. One may then calculate the P value as 1 minus the fractional reduction.

If the type of windbreak desired does not correspond to one tested in the study, its AI parameter may be estimated by multiplying the AI value of the most similar windbreak that was tested by a parameter ratio. A parameter ratio is calculated using the test series results in the study as described in the pertinent section of the report (use the table of contents and list of figures) dealing with a parameter which is non-standard in the user's windbreak. It is given by:

$$PR = \frac{\text{AI (user value of parameter)}}{\text{AI (parameter value for similar windbreak used in study)}}$$

Thus to use an open row windbreak located 120 feet upstream of the house in which the trees are 10 feet tall, one uses the AI for an open row at 120 mf upstream (see Figure 26 in the Distance and Repeatability Series Section), and multiplies it by the ratio of the AI of the open row 10 mf tall over the AI of the open row 25 mf tall, the same height as the open row used in the distance tests. These numbers can be obtained from Figure 38 in the Height Variation and Row Staggering Series. The problems of non-standard drag coefficient, tree spacing, house/tree separation, etc. may all be taken care of by referring to the appropriate results, matching the desired windbreak as closely as possible with a tested configuration, and then making up the differences with Parameter Ratios.

4.1 SPECIAL CASES

In regard to the variation of AI with tree height, both curves derived in the tree height series are basically similar and in conjunction form a good first order polynomial function of AI on tree height. This function is given by:

$$AI(ht) = \min((1.02), (-.015\ ht - 1.115))$$

where ht is the tree height in [model] feet.

Since the windbreak protection is independent of tree spacing along the direction of the windflow over a broad range, windbreak rows planted at an angle with respect to the windflow direction may be treated as a windbreak row whose row density is given by:

$$RD_{eff} = \frac{RD_{actual}}{Sin\ \Theta}$$

where RD is the effective row density in trees per foot, RD(actual) is the actual tree row density, and theta is the angle the windbreak row makes with the direction of windflow. The AI of the effective windbreak row may then be calculated using parameter ratios.

Houses near a forest or other dense tree stand may assume the AI reduction of any direction in which the stand lies upstream of the house to be 95% if the forest is five or more rows deep. For stands of forest (as opposed to open grown) trees that are not deep, the homeowner should take the results of the underpruning test, use a parameter ratio to position the downstream row at the correct distance from the house, and another PR from the incremental row tests to compensate for the number of rows in the stand. For stands of greater than three rows, AI may be decreased by the difference of the AI value for two rows and the value for three rows as seen in the Incremental Row Series results.

4.2 SAMPLE APPLICATONS

Consider an average middle class home located in a recently developed subdivision consisting of from 200 to 300 3/4 acre lots. The subdivision is located in the Trenton area. This kind of subdivision is typically a former farm field, so the terrain is fairly flat with very few trees. The home is basically a two story box similar to the one in the study. It is situated in the center of a lot that is 180 ft square. Its front and back yards are 77.5 ft deep, and its side yards are 72.5 feet deep. These depths are important information, as they place limitations on the possible house/windbreak separations.

The house is of modern construction with average floor area, and is poorly insulated. The heating bill is $600 dollars for the heating season. The homeowner, desiring to reduce heating costs through the use of trees, calls the nearby landscape contractor to find out that he can have 6 foot tall cedar or spruce trees planted for $60 per tree. His problem is to determine the planting arrangement that will afford him the most protection.

In the Trenton area, the prevailing winter winds are from the northwest. One approach to the problem is to plant a windbreak that will protect the house only from winds from this direction. A leading wedge located in the northwest corner of the lot at a distance of 10 feet from the property lines would be spaced about 90 feet from the house corner. Neglecting the minor deviations due to house angle, Figure 48 indicates that 25 foot trees in this position would provide an AI that is 49% of the same situation without trees when the wind blows from the northwest. However, since the trees are initially only six feet tall, one computes the parameter ratio from the AI(ht) function in the Special Cases section above to be 1.385. The percent of unprotected AI is therfore 68%, so P=.68 for the northwest direction, and remains one for the other seven. Using the summation formula for heat loss, it is found that the three trees save the homeowner $19.52 the first year. At this rate it would take 9.2 years to payback the $180 initial investment on the trees. However, spruce and cedar trees grow at about one foot per year, and the homeowner will save more and more each year as his trees grow. At the end of 20 years, his seasonal savings have grown to $29.42 due to tree growth. Taking into account the growth of trees drops the payback period to 8.4 years. If one takes into consideration an inflation rate of 7% per year, thenthe investment will be repaid in 7 years.

To protect the home from wind blowing from all directions, the home owner might use a contour box arrangement, possibly moving it near to the lot perimeter to increase its effect (see Contour Box Series). The percent of unprotected AI for a Contour Box located at 30 feet from the house perimeter is 76%. However, when the Contour Box is spread to 60 feet from the house perimeter (very near to the edge of the lot), the parameter ratio reduces this to 68.4%. After applying the parameter ratio for 6 versus 25 foot trees, the percent AI rises back to 94.7%. Using P=.947 for all 8 directions in the Heat Loss Summation equation, the total heat savings for the first year are $10.06. To pay back the $2100 investment for 35 trees (the perimeter and therefore the number of trees in the contour box increases with house/tree separation if the tree row density is maintained constant) would take just over 38 years considering tree growth, or 25 years including the effects of 7% inflation. The contour box, however, does save more money in the long run. At the end of 50 years, if the homeowner planted the leading wedge arrangement, he has netted $15,374 for his efforts, or about $307 a year. The contour box in 50 years will have yielded a net $38,775, or $775 a year. The planting of trees to save energy is similar to making an investment. One can either opt for a short term maturity with a lower interest rate, or a long term investment which yields higher gains.

The Trenton area is characterized by variable winds, although there is a definite prevailing wind. In areas where there is a more or less constant prevailing wind of high speed, a selective windbreak planting method such as the leading wedge would be more effective. The wind characteristics of the geographic area, the level of initial investment, and the payback period desired are of key importance in determining the optimum planting configuration.

The technique described above can be used to predict the effectiveness of a given windbreak requiring only the results of this study, simple mathematics, and easily obtainable information about the local area. It is now possible for anyone to predict the monetary savings to be derived from the planting of trees without costly equipment. It is hoped that the availability of this information will encourage the planting of windbreaks, which have been shown by this study to be economically sound as energy conservers, as well as being aesthetically pleasing.

5. CONCLUSIONS

It has been shown that trees reduce air infiltration in housing by converting directed kinetic energy in the approaching wind into random turbulent energy by passing air through tortuous paths in their crowns. The functioning of trees as bluff bodies has been shown to be minimal for naturally occurring trees. Protection from wind is improved by any action that increases the amount of tree crown matter upstream of the protected structure. This is also due to the fact that air infiltration into a building seems to be caused by pressure gradients on windward walls, with leeward walls remaining very close to interior pressure.

Techniques for energy conservation through the use of trees that call for trees being planted so as to channel the flow of air away from a house, or to block air from striking a house, or planting trees downstream of a leeward wall of a building to balance exterior pressures on that building have been shown to be ineffective.

To provide maximum sheltering effect, any tree windbreak should be planted at least 45 feet upstream of the building it protects to give the turbulence generated by the tree crowns a chance to develop. By contrast, bushes and other low profile windbreaks are best used in close proximity upstream of the building they protect, so that they extend the stagnation zone on the upstream wall and cause the approaching wind to flow over the building in a smooth manner.

On a short term basis, it is more cost effective to plant windbreaks that selectively protect against the worst winds of a region. These windbreaks should consist of as few trees as possible.

If one is thinking of a long term investment, it is more desirable to heavily protect the structure, since the trees planted eventually grow large and become quite efficient in providing wind protection.

In the Trenton area, fuel savings averaging 3.1% over twenty years were estimated using three trees to protect against prevailing winds. Using a more extensive planting pattern affording general protection, average fuel savings of 14.6% over 50 years have been shown. A tree payback period of as short as 7 years using three trees to protect against prevailing winds has been shown. The economy of tree planting to save energy has been decidedly demonstrated.

The dearth of accurate information on the aerodynamic behavior of trees is noted, and it is concluded that further study of the wind behavior of full size trees is needed. The behavior of complex windbreak planting configurations may be deduced from knowledge of wind behavior of individual trees in the windbreak.

It is further concluded that windtunnel modelling is an efficacious way of studying the behavior of windbreaks, and that further windtunnel study of shelterbelt behavior is desirable.

BIBLIOGRAPHY

Bates, C. G., "Shelterbelt Influences II, The Value of Shelterbelts in House Heating", Journal of Forestry, V. 43, No. 3, pp. 176-196, March 1945

Bean, A., Alpere, R. W., and Federer, C. A., "A Method for Categorizing Shelterbelt Porosity", Agricultural Meteorology, 1975, V. 14, pp. 417-429

Buckley, C. E., "A Catalog of Test Pressure Coefficient Distributions for Use with the Optimum Use of Coniferous Trees Study", Center for Environmental Studies Draft Report, January 1978

Chaney, T., Golden, F., Maxwell, L. and Rogers, J., "A Natural Resource Inventory of the Stoney Brook Watershed, Mercer and Hunterdon Counties, New Jersey", A Master of Regional Planning Report for the Graduate School of Fine Arts, University of Pennsylvania, 1974

Fraser, A. J. and Walshe, D. E., "Wind Tunnel Tests on a Model Forest", National Physical Laboratory (U. K.) Aero Report /1078, October 1973

Flemer, W., "The Role of Plants in Today's Energy Conservation", American Nurseryman Magazine, May 1, 1974

Harrje, D. T., "Retrofitting: Plan, Action and Early Results Using the Townhouses at Twin Rivers", Center for Environmental Studies Report No. 29, June 1976

Heisler, G. M., "How Trees Modify Metropolitan Climate and Noise, Forestry Issues in Urban America", Proceedings 1974 National Convention of the Society of American Foresters, New York, September 22-26, pp. 103-122

Hsi, G. and Nath, J. H., "A Laboratory Study on the Drag Force Distribution Within Model Forest Canopies in Turbulent Shear Flow", Fluid Mechanics Program, College of Engineering, Colorado State University, Report No. CER67-68GH-JHN50, Fort Collins, March 1968

Marshall, R. D., "A Study of Wind Pressures on a Single Family Dwelling in Model and in Full Scale", NBS Technical Note 852, October 1974

Mattingly, G. E., Harrje, D. T., and Heisler, G. M., "On the Effectiveness of Evergreen Windbreaks for Reducing Residential Energy Consumption", CES Draft Report, August 1977

Mattingly, G. E. and Peters, E. F., "Wind and Trees - Air Infiltration Effects on Energy in Housing", Center for Environmental Studies Report No. 20, May 1975

Meroney, R. N., "Characteristics of Wind and Turbulence in and above Model Forests", Journal of Applied Meteorology, 1968, V. 7, pp. 780-788

Miller, D. R., Rosenberg, N. J., and Bagley, W. T., "Wind Reduction by a Highly Permeable Tree Shelterbelt", Agricultural Meteorology, 1975, V. 14, pp. 321-333

Peterka, J. and Cermak, J., "Simulation of Atmospheric Flows in Short Wind Tunnel Test Sections", Fluid Dynamics and Diffusion Laboratory, Report No. CER73-74JAP-JEC12, Colorado State University, June 1974

Petrides, G. A., A Field Guide to Trees and Shrubs, Houghton Mifflin Company, Boston, 1972

Plate, E. J., Aerodynamic Characteristics of Atmospheric Boundary Layers, Atomic Energy Commision, Oak Ridge, 1972

Pope, A. and Harper, J. J., Low Speed Wind Tunnel Testing, Wiley, New York, 1966

Raymer, W. G., "Wind Resistance of Conifers", National Physical Laboratory (U. K.) Aero Report /1008, April 1962

Roberson, J. A. and Crowe, C. T., Engineering Fluid Mechanics, Houghton Mifflin Company, Boston, 1975

Sadeh, Willy Z., "Weather-Climate Modelling for Real Time Applications in Agriculture and Forest Meteorology", Preprints from Thirteenth Conference on Agriculture and Forest Meteorology, West Lafayette, Indiana, April 4-6, 1977

Saqi, R. and Seginer, I., "Drag on a Windbreak in Two Dimensional Flow", Agricultural Meteorology, 1971/1972, V. 9, pp. 323-333

Woodruff, N. P., "Shelterbelt and Surface Barrier Effects on Wind Velocities, Evaporation, House Heating, and Snowdrifting", Technical Bulletin 77, Agricultural Experiment Station, Kansas State College at Manhattan, December 1954

LIST OF FIGURES

APPENDIX 1: AI PARAMETERS FOR EACH TEST RUN

NO.	NAME	DESCRIPTION	AI
1	HS0	HOUSE ALONE	1.020
2	HS45	HOUSE ALONE,HA=45	1.189
3	HS90	HOUSE ALONE,HA=90	1.065
4	HS0Q1	HOUSE ALONE,Q=1	1.055
5	HS0Q2	HOUSE ALONE,Q=2	1.022
6	HS0Q3	HOUSE ALONE,Q=3	1.009
7	STHT15	SINGLE TREE,HT=15	.914
8	STHT30	SINGLE TREE,HT=30	.824
9	STHT45	SINGLE TREE,HT=45	.746
10	STHT60	SINGLE TREE,HT=60	.708
11	STHT75	SINGLE TREE,HT=75	.767
12	STHT90	SINGLE TREE,HT=90	.743
13	STHT120	SINGLE TREE,HT=120	.758
14	STHT150	SINGLE TREE,HT=150	.792
15	STHT180	SINGLE TREE,HT=180	.856
16	STHT210	SINGLE TREE,HT=210	.856
17	STHT240	SINGLE TREE,HT=240	.859
18	STSD0	SINGLE TREE,SD=0	.807
19	STSD4	SINGLE TREE,SD=-4	.868
20	STSD12	SINGLE TREE,SD=-12	.945
21	STSD20	SINGLE TREE,SD=-20	1.021
22	STSD28	SINGLE TREE,SD=-28	1.010
23	STSD36	SINGLE TREE,SD=-36	1.007
24	STSD44	SINGLE TREE,SD=-44	1.023
25	ORHT15	OPEN ROW,HT=15	.796
26	ORHT30	OPEN ROW,HT=30	.711
27	ORHT45	OPEN ROW,HT=45	.664
28	ORHT60	OPEN ROW,HT=60	.640
29	ORHT75	OPEN ROW,HT=75	.623
30	ORHT90	OPEN ROW,HT=90	.615
31	ORHT120	OPEN ROW,HT=120	.632
32	ORHT150	OPEN ROW,HT=150	.639
33	ORHT180	OPEN ROW,HT=180	.654
34	ORHT210	OPEN ROW,HT=210	.649
35	ORHT240	OPEN ROW,HT=240	.667
36	HRHT15	HEDGEROW,HT=15	.631
37	HRHT60	HEDGEROW,HT=60	.374
38	HRHT90	HEDGEROW,HT=90	.371
39	HRHT120	HEDGEROW,HT=120	.313
40	HRHT180	HEDGEROW,HT=180	.358
41	HRHT228	HEDGEROW,HT=228	.338
42	ORHA45	OPEN ROW,HA=45	.836
43	ORHA90	OPEN ROW,HA=90	.749
44	HRHA45	HEDGEROW,HA=45	.467
45	HRHA90	HEDGEROW,HA=90	.444
46	OR	OPEN ROW	.747
47	ORM2	OPEN ROW,NT=4	.711
48	ORM4	OPEN ROW,NT=2	.753
49	HR	HEDGEROW	.494
50	HRM2	HEDGEROW,NT=10	.475
51	HRM4	HEDGEROW,NT=8	.513
52	HRM6	HEDGEROW,NT=6	.507
53	ORSD1	OPEN ROW,CD=.43	.806
54	ORSD3	OPEN ROW,CD=.66	.613

APPENDIX 1 (CONTINUED)

NO.	NAME	DESCRIPTION	AI
55	ORSD4	OPEN ROW,CD=.72	.593
56	ORSD12	OPEN ROW,CD=.92	.337
57	SPLL1	SPECIAL,TPMF=.0722	.671
58	SPLL2	SPECIAL,TPMF=.0913	.628
59	SPLL5	SPECIAL,TPMF=.0650	.700
60	SPLL7	SPECIAL,TPMF=.0514	.795
61	SPLL8	SPECIAL,TPMF=.0389	.875
62	SPTH15	OPEN ROW, TH=15	.924
63	SPTH20	OPEN ROW, TH=20	.792
64	SPTH30	OPEN ROW, TH=30	.578
65	SPTH40	OPEN ROW, TH=40	.541
66	SGTH15	STAGGERED OPEN ROW,TH=15	.926
67	SGTH20	STAGGERED OPEN ROW,TH=20	.750
68	SGTH25	STAGGERED OPEN ROW,TH=25	.800
69	SGTH30	STAGGERED OPEN ROW,TH=30	.606
70	SGTH40	STAGGERED OPEN ROW,TH=40	.543
71	INCR1	MULTI-ROW	.580
72	INCR2	MULTI-ROW	.439
73	INCR3	MULTI-ROW	.535
74	INCR4	MULTI-ROW	.370
75	UPRN20	OPEN ROW,TS=20,TT=RC	1.091
76	UPRN15	OPEN ROW,TS=15,TT=RC	1.033
77	UPRN10	OPEN ROW,TS=10,TT=RC	1.087
78	UPRN5	OPEN ROW,TS=5,TT=RC	.950
79	UPRN0	OPEN ROW,TS=0,TT=RC	.698
80	UPRNM3	OPEN ROW,TS=-3,TT=RC	.602
81	FA3015	OPEN ROW,HT=30,-15	.710
82	FA3030	OPEN ROW,HT=30,-30	.728
83	FA3045	OPEN ROW,HT=30,-45	.691
84	SR3030	OPEN ROW,HA=90,TA=90,HT=30,-30	1.127
85	SR1515	OPEN ROW,HA=90,TA=90,HT=15,-15	.975
86	SR4545	OPEN ROW,HA=90,TA=90,HT=45,-45	1.131
87	SR30	OPEN ROW,HA=90,TA=90,HT=-30	1.075
88	CB0	CONTOUR BOX,HT=30 ALL AROUND,HA=0	.762
89	CB45	CONTOUR BOX,HT=30 ALL AROUND,HA=45	.778
90	CB90	CONTOUR BOX,HT=30 ALL AROUND,HA=90	.793
91	LW30	LEADING WEDGE,HT=15	.655
92	LW45	LEADING WEDGE,HT=30	.550
93	LW60	LEADING WEDGE,HT=45	.512
94	LW75	LEADING WEDGE,HT=60	.501
95	LW90	LEADING WEDGE,HT=75	.477
96	LW120	LEADING WEDGE,HT=105	.482
97	LW150	LEADING WEDGE,HT=135	.541
98	LW180	LEADING WEDGE,HT=165	.542
99	LW210	LEADING WEDGE,HT=195	.629
100	LW240	LEADING WEDGE,HT=225	.659
101	SPDW1	DRIVEWAY, MAIN ROW HT=60	.740
102	SPDW2	DRIVEWAY, MAIN ROW HT=60	.381
103	SPDW3	DRIVEWAY, MAIN ROW HT=60	.483
104	SPDW4	DRIVEWAY, MAIN ROW HT=60	.463
105	SPDW5	DRIVEWAY, MAIN ROW HT=60	.349
106	SPDW6	DRIVEWAY, MAIN ROW HT=60	.571
107	SPDW7	DRIVEWAY, MAIN ROW HT=60	.356
108	SPDW8	DRIVEWAY, MAIN ROW HT=60	.287

APPENDIX 2: TREE SHAPES SURVEYED

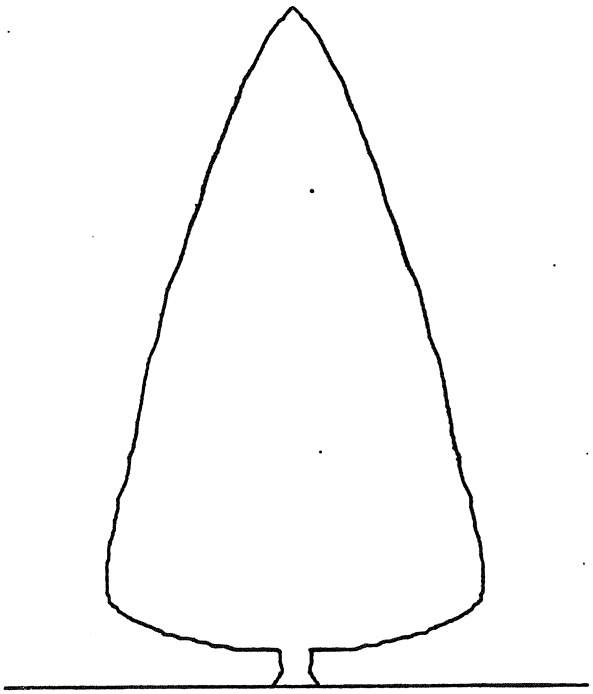

NORWAY SPRUCE

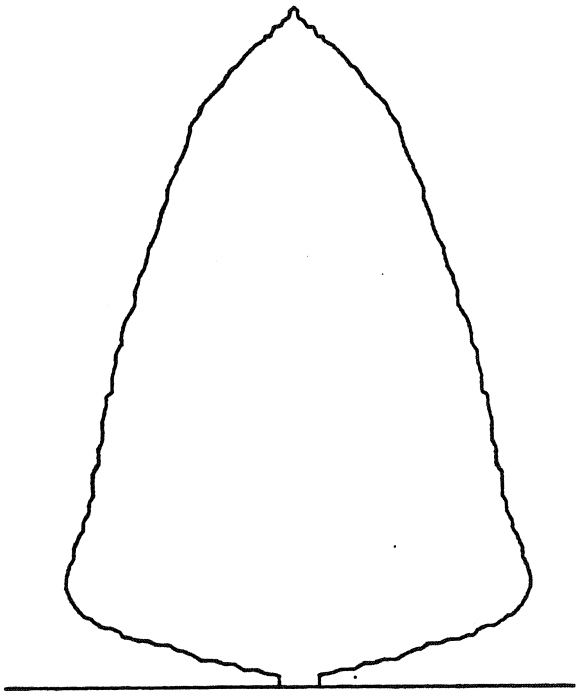

COLORADO BLUE SPRUCE

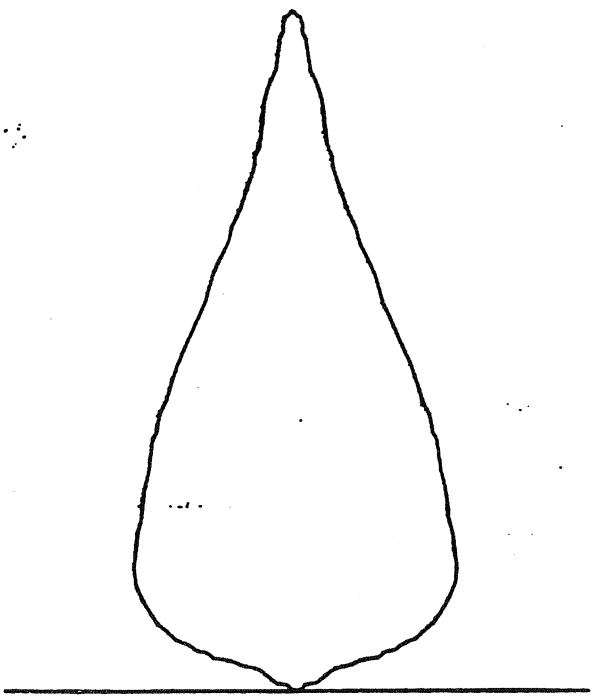

RED SPRUCE

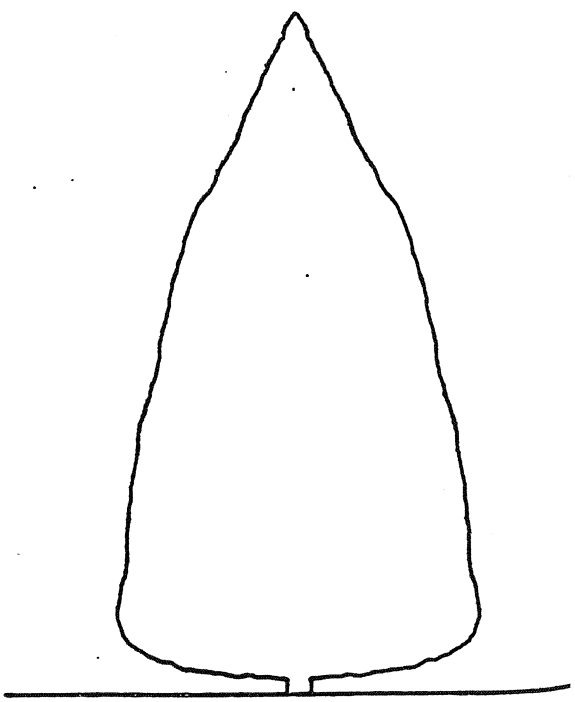

WHITE SPRUCE

SPRUCES

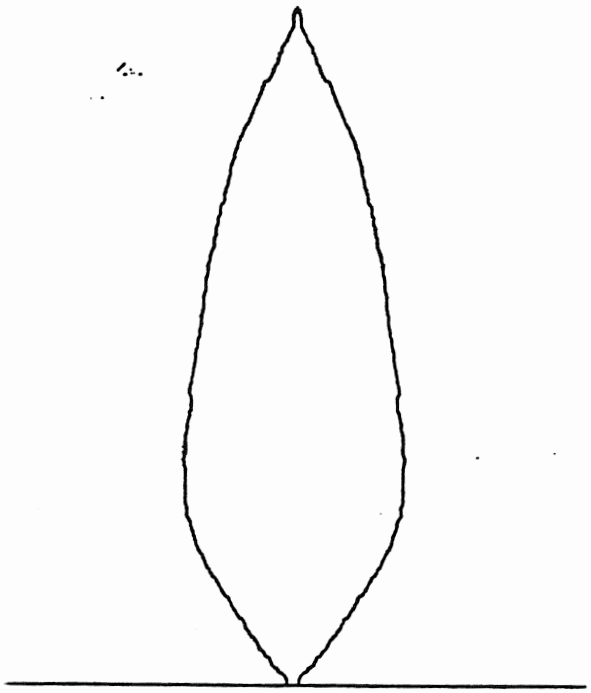

RED CEDAR

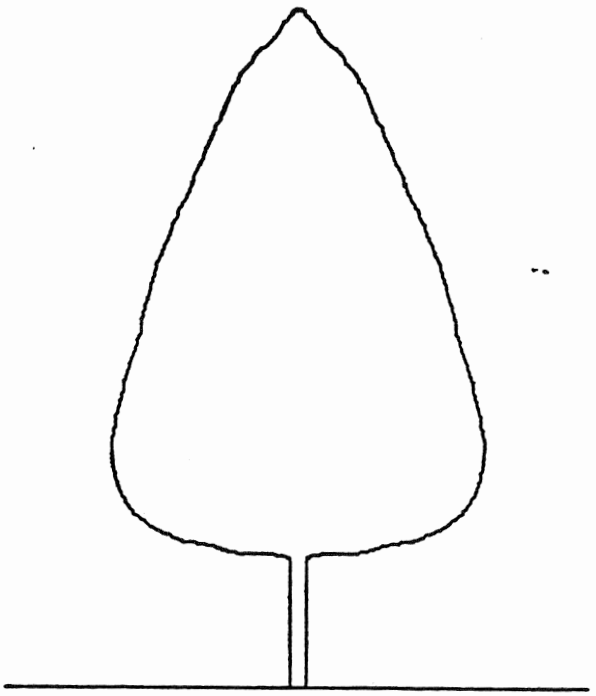

UNDERPRUNED RED CEDAR

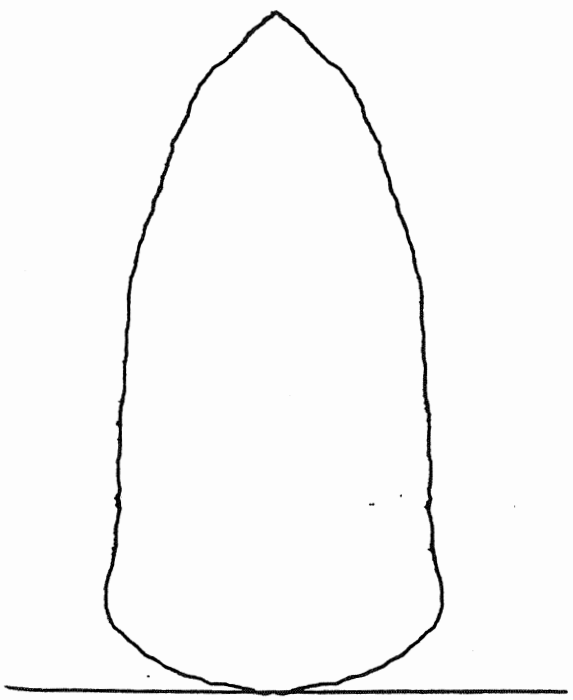

TLANTIC WHITE CEDAR

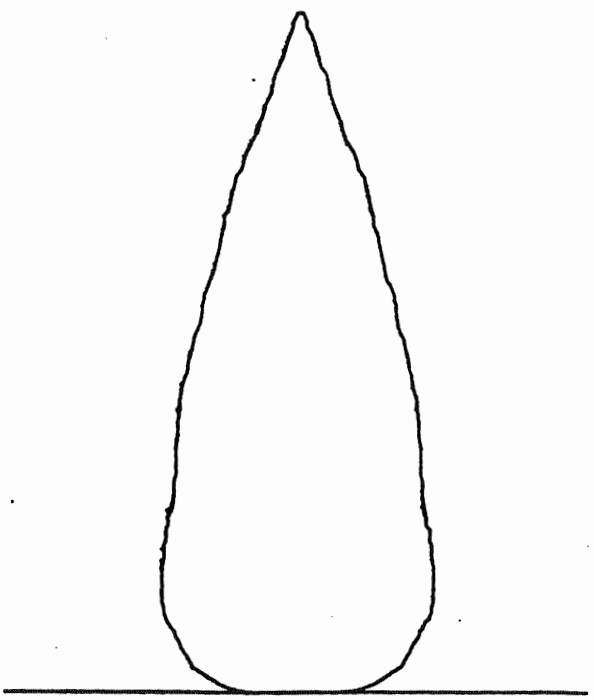

ARBOR VITAE

CEDARS

APPENDIX 3: INSTRUCTIONS FOR USE OF CATALOG OF TEST PRESSURE COEFFICIENT DISTRIBUTIONS AND SAMPLE DATA PAGE

The pressure coefficient distribution plots found in the Catalog of Test Pressure Coefficient Distributions (CTPD) were used in determining the results reported in "The Optimum Use of Coniferous Trees in Reducing Home Energy Consumption". These plots, while not being necessary to the understanding or use of "The Optimum Use . . . " are available in the CTPD so that they might be used to understand the actual wind pressures on a dwelling under the many configurations tested.

The data for each test is plotted on a separate page. There are five sections to each page, numbered (1)-(5) on the sample test page showing the data for test 1. Section 1, the top diagram, is a plan view of the model configuration in the wind tunnel. The wind flows in the direction of the arrow indicated by the word "WIND". A second, smaller arrow is drawn on the house roof. This shows the house direction vector, which is repeated in sections (2) and (3), where it is sc marked.

By visually matching the house direction vector between the plan view in section (1) and the vertical pressure coefficient distribution plot group in section (2), it can be determined that the plot on the right of section (2) is

that of the upstream wall in test 1, the plot on the left is that of the downstream wall, and that the roof plots fall into place in an intuitively logical manner. The pressure coefficient distribution plots for the side walls of the house are both superimposed and plotted within the actual house silhouette in section (2). The distribution of the wall which faces into the page is plotted the same as all the other distributions, but the wall which faces out of the page is plotted as a series of unconnected dots.

Visually matching the house direction vector between section (1) and the Horizontal Pressure Coefficient Distributions in section (3) defines the surfaces to which each of those plots refer.

The ordinate units of the plots are non-dimensional, being the pressure coefficients defined in "The Optimum Use . . . ". Since the abcissa distance units are scaled pictorially to the size of the house silhouettes, they are also not assigned units.

Section (4) is the descriptive label of the test consisting of the test number, the test name in parentheses, and a descriptive field. This information, along with the AI for the test, may also be found in Appendix 1 of "The Optimum Use . . . ". In many of the descriptive fields, various parameters are used in the format parameter=keyword. Following is a list of the parameters used, their meanings, and default values used in those tests for which they are

not specified. The units of the parameters are the same as those of their default values.

1. HA - house angle, the angle between the vector normal to the plane of the front wall (the wall facing the same way as the house direction vector) and the direction of windflow. Default=0 degrees.

2. Q - ambient dynamic pressure in the wind tunnel, default= 2 inches of water.

3. HT - house/windbreak row separation. Default=30 model feet. If more than one value is given, then more than one windbreak row was used. Negative numbers refer to tree rows located downstream of the house.

4. SD - the sideways (perpendicular to windflow direction) displacement of a tree off of directly upstream of a house. Negative numbers refer to displacements to the right when facing upstream. Default=0 model feet.

5. NT - the number of trees in a windbreak row. Defaults: single tree=1, open row=6, Hedgerow=12

6. CD - the drag coefficient of the trees used in the windbreak configuration. Default=.58.

7. TPMF - trees per model foot, an indication of the planting density of a windbreak row. Defaults: open row=.0600, Hedgerow=.1282.

8. TH - tree height. Default=25 model feet.

9. TS - trunk size, applies only to undepruned red cedar tests. Indicates variation off normal trunk height. Positive numbers indicate a longer trunk, while shorter trunks are indicated by negative numbers. Default=0 model feet.

10. TT - tree type, either RC (red cedar) or the default NS (Norway spruce), indicates the tree silhouette after which the model was constructed. See Appendix 2 in "The Optimum Use . . . ".

11. TA - tree row angle, the angle of a vector normal to a windbreak row and based in the plan view center of the house with the oncoming wind direction vector. Default=0 degrees.

Section (5) is the AI parameter calculated for the test, also found in Appendix 1 of "The Optimum Use . . . ".

(1)

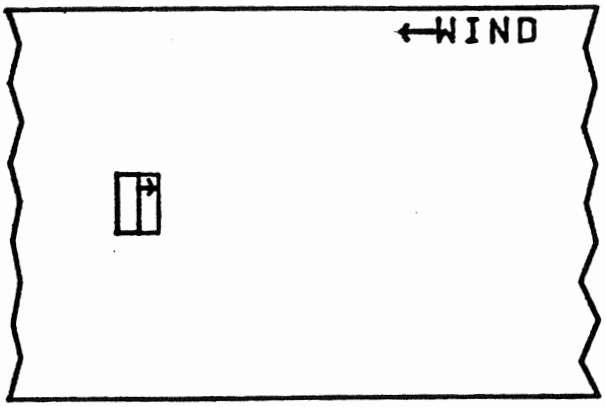

(2)

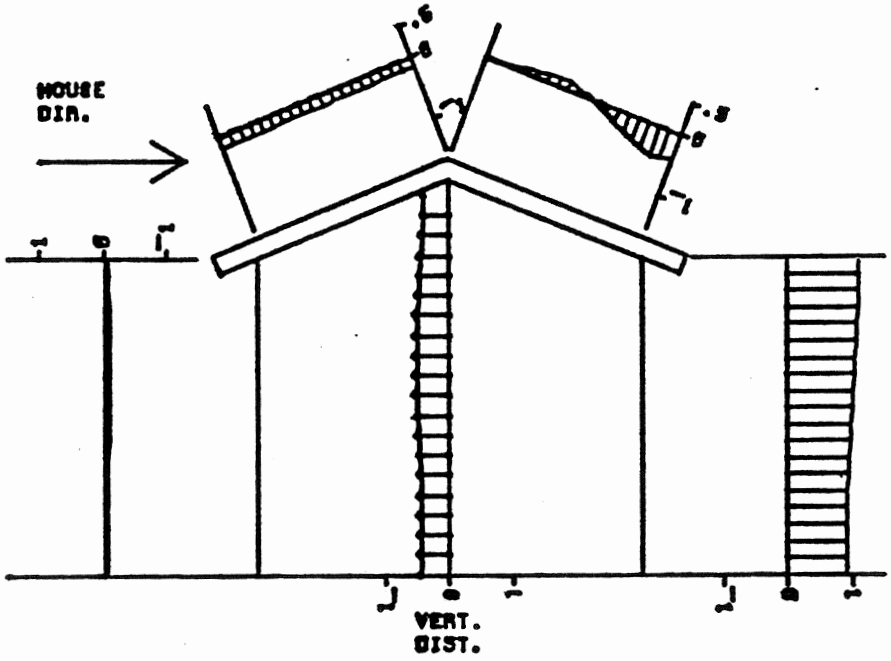

(3)

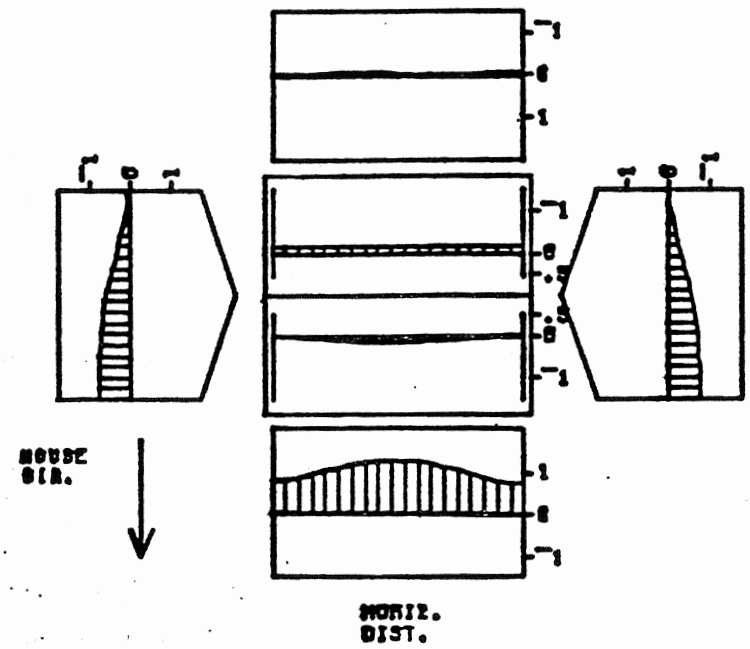

(4)

TEST 1 (HS0) : HOUSE ALONE

(5)

AI= 1.020